the
abdus salam
international
centre
for theoretical
physics

united nations
educational, scientific
and cultural
organization

international atomic
energy agency

preprint

GROUP VELOCITY TOMOGRAPHY AND REGIONALIZATION IN ITALY AND BORDERING AREAS

A. Pontevivo

and

G.F. Panza

33/05

IC/2001/136

United Nations Educational Scientific and Cultural Organization
and
International Atomic Energy Agency

THE ABDUS SALAM INTERNATIONAL CENTRE FOR THEORETICAL PHYSICS

GROUP VELOCITY TOMOGRAPHY AND REGIONALIZATION IN ITALY AND BORDERING AREAS

A. Pontevivo
Department of Earth Sciences, University of Trieste, Trieste, Italy

and

G.F. Panza
Department of Earth Sciences, University of Trieste, Trieste, Italy
and
The Abdus Salam International Centre for Theoretical Physics, SAND Group, Trieste, Italy.

MIRAMARE – TRIESTE

October 2001

Abstract

More than one hundred group velocity dispersion curves of the fundamental mode of Rayleigh waves have been processed to obtain tomographic maps, in the period range from 10 s to 35 s, for the Italian peninsula and bordering areas. We compute average dispersion relations over a 1°x1° grid, and, since the lateral resolving power of our data set is of about 200 km, we group the cells of the grid accordingly to their dispersion curves. In this way and without any a priori geological constraints, we define seven different regions, each characterised by a distinctive mean group velocity dispersion curve. The resulting regionalization can be easily correlated with the main tectonic features of the study area and mimics a recently proposed structural sketch. Average models of the shear wave velocity in the crust and in the upper mantle for a few selected regions are presented. The very low S-wave velocity values found in the uppermost upper mantle of the Southern Tyrrhenian basin are consistent with a large percentage of partial melting, well in agreement with the presence of the Vavilov-Magnaghi and Marsili huge volcanic bodies.

1. Introduction.

The present setting of the Italian peninsula and surrounding areas is controlled by a quite complex system of geodynamic processes. It isn't only the result of the N-S shortening between Africa and Europe, but of a more complex plate interaction. The current extensional deformations in Italy and the thrusting in its northern part depict the deforming margins of the relatively aseismic Adriatic area (Anderson and Jackson, 1987). Other geodynamic processes must be taken into account, as described by Meletti et al. (2000) in their seismotectonic model of the Italian peninsula and surrounding areas: the anticlockwise rotation of Adria microplate versus Europe with the rotation pole located in Northern Italy; the shallow asthenospheric wedges in the Northern Apenninic Arc and Calabrian Arc; the Alps-Dinarides convergence with development of compressive-transpressive features along the plate margin; the compression fronts of the Adria-verging outer thrust systems (Southern Alps and Dinarides); the compression fronts of the Adria-verging inner thrust systems (Northern Apenninic Arc and Calabrian Arc) and the inactive compression front in the Southern Apennines; the extensional young fault system between Adria and Europe in the Southern Apennines; the Wadati-Benioff zone of the Southern Tyrrhenian Sea.
In this work we focus on the Italian peninsula, its bordering seas (Southern Tyrrhenian Sea, Adriatic Sea, Ionian Sea), the area of the Dinarides chain and a continental part of Greece, to differentiate the gross features of the crust and lid, in terms of S-wave velocity and thickness of the layers, through surface wave tomography and non-linear inversion.

2. The Method.

To extract the group velocity of the fundamental mode of Rayleigh wave, we have analysed, by the Frequency-Time ANalysis (called FTAN) developed by Levshin et al. (1972, 1992), more than one hundred vertical component seismograms (Table A.1 in Appendix A).

Figure 1: Paths from epicenter (●) to station (▲) on the study area.

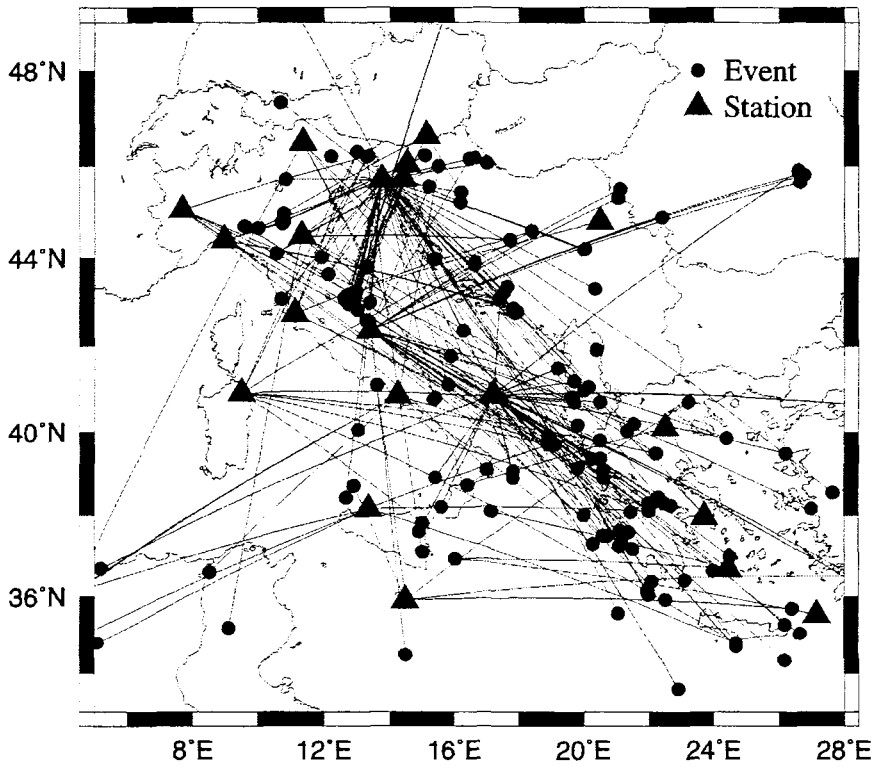

Table 1: List of Code, Latitude and Longitude of recording stations.

Code	Station	Latitude	Longitude	Code	Station	Latitude	Longitude
TRI	Trieste	45.709N	13.764E	NPL	Napoli	40.846N	14.257E
AQU	Aquila	42.354N	13.405E	GSO	Grosseto	42.752N	11.116E
GENL	Genova	44.405N	08.969E	TNO	Torino	45.058N	07.697E
MIL	Milos	36.680 N	24.440 E	BOL	Bologna	44.490N	11.329E
KAP	Karpathos	35.550 N	27.170 E	OLB	Olbia	40.926N	09.495E
LIT	Litochoro	40.100 N	22.490 E	BLZ	Bolzano	46.504N	11.346E
LJU	Ljubljana	46.0438N	14.527E	PAL	Palermo	38.143N	13.347E
BISS	Branik Nad Muto	46.6478N	15.1272E	BAI	Bari	40.877N	17.203E
CEY	Cerknica	45.7388N	14.4267E	MLT	Malta	35.900N	14.480 E
BGY	Beograd	44.802N	20.515E				

The stations used are located in Italy, Greece and Slovenia and are listed in Table 1. To these data we have added other relevant group velocity measurements (see Tables A.2 and A.3 in the Appendix A) available in the literature (Mantovani et al., 1985; Calcagnile et al., 1982; Farrugia and Panza, 1981; Yanovskaya et al., 1990) and all the considered epicenter-station paths are shown in Fig.1. The available dispersion measurements have been used to perform surface-wave tomography, in the period range from 10 s to 35 s, following the method developed by Ditmar and Yanovskaya (1987) and Yanovskaya and Ditmar (1990).

The tomographic maps, presented in Fig.2, have been discretized with a 1°x1° grid and for each cell of the grid we have computed a local average group velocity curve. We have grouped the cellular dispersion curves considering similar the curves of adjacent cells if, at each considered period, they differ from their mean group velocity value by less than two standard deviation. A phase-wave tomography is performed, in the period range from 30 s to 100 s, following the same method using phase velocity data (see Table B.1 in the Appendix B) available in literature. By the non-linear inversion, known as hedgehog method (Valyus et al., 1969; Valyus, 1972; Knopoff, 1972), of the obtained average group and phase velocity curves, using as a priori information what is available in the literature to fix the uppermost part of the crust, few average lithospheric models in the study area are obtained.

2.1 Data and Frequency-Time ANalysis (FTAN).

Tomographic methods applied to dispersion measurements are often used in studies of the crust and upper mantle (Ritzwoller et al., 1998; Vuan et al., 2000; Yanovskaya et al., 1988; Yanovskaya et al., 1998; Yanovskaya and Antonova, 2000; Yanovskaya et al., 2000; Pasyanos et al., 2001; Karagianni et al., 2001). One fundamental requirement to produce reliable tomographic images is the rather uniform distribution, in different directions, of the paths sampling the study area and from this the importance to collect data to obtain a good path-coverage.

Most of the processed events (Table A.1 in the Appendix A) are located in the Italian peninsula and bordering areas: Adriatic, Ionian and Tyrrhenian seas, Greece, Croatia and Albania. The magnitude of the events, generally larger than 4.0 Ms, is taken from NEIC bulletins, as well as their locations and origin times used to measure group velocity. The event-station paths lengths are in the range from about 140 km to 1200 km. Rayleigh wave

group velocity dispersion curves have been measured from the vertical component records, using the FTAN method (Levshin et al., 1972; Levshin et al., 1992).

From Fig.1 it is seen that the paths distribution is rather homogeneous over the whole Italian peninsula, in the Tyrrhenian Sea and in and around the Adriatic and Ionian seas. The period range common to most of the dispersion curves is 10-35 s, thus, in this range, with a step of 5 s, we have constructed the tomographic maps shown in Fig.2.

2.2 Tomography of group velocity.

Surface waves dispersion measurements along different paths are widely used to study lateral variations and anisotropy of the lithospheric structure, to map local values of the velocities for a set of periods and to determine related vertical velocity distribution in the area under investigation. Thus, we use the two-dimensional tomography approach developed by Ditmar and Yanovskaya (1987) and Yanovskaya and Ditmar (1990) which is a generalisation to two dimensions of the classical one-dimensional method of Backus and Gilbert (e.g., Backus and Gilbert, 1968 and 1970).

We outline the method for the general inverse problem for the travel times using Cartesian coordinates (x, y) in a plane. The two-dimensional problem on a spherical surface may be reduced to the case of a plane by the Mercator transformation of the coordinates and transformation of the velocity (Yanovskaya, 1982; Yanovskaya et al., 1988). The general approach for solving the plane and the spherical problem is the same, but the functions used to represent the solution are different in the two cases. If the given data are the phase and/or group velocities at different periods and along some paths, crossing the region under investigation, and if we want to determine a function which fits the data, the general two-dimensional tomography problem can be formulated as follows (Yanovskaya and Ditmar, 1990):

- the input data set are the travel times t_i (i= 1, 2 , ..., N) along different paths L_i, which are assumed to be straight lines[1];
- the data are affected by experimental errors ε_i described by the covariance matrix R_t (e.g. Lay and Wallace, 1995);

[1] The validity of this assumption, in our case, has been successfully tested numerically as suggested by Yanovskaya et al. (1998) by computing, for each assumed straight path, the curved path, consistent with the pattern of the phase velocity distribution, representative of the study region.

- it is assumed a starting model with the velocity values V_0, where the travel times t_{0i} along each path are calculated;
- the travel time residuals are defined as $\delta t_i = (t_i - t_{0i}) = \int_{L_{0i}} m(x,y) V_0^{-1} ds + \varepsilon_i$ where L_{0i} is a segment of the path and the relative slowness correction is defined as $m(x,y) = (V^{-1}(x,y) - V_0^{-1}) / V_0^{-1}$, with the assumption that the lateral velocity variations are small, $|m(x,y)| << 1$.
- The function $m(x,y)$ is assumed to be smooth, and it is determined by minimising the functional:

$$(\boldsymbol{\delta t} - \mathbf{Gm})^T (\boldsymbol{\delta t} - \mathbf{Gm}) + \alpha \int_S |\nabla m|^2 dxdy \quad (1)$$

where $(\mathbf{Gm})_i = \int_S G_i(x,y) m(x,y) dxdy = \int_{L_{0i}} m(x,y) V_0^{-1} ds$, S is an area including all paths, which is assumed to be the whole plane, and α is a parameter of regularisation[2].

- On the contour C_S of the area S (at infinity) :

$$(\partial m / \partial n)_{C_S} = 0 \quad (2)$$

It follows from equations (1) and (2) that

$$m(x,y) = \sum_{i=1}^{N} \lambda_i \psi_i(x,y) + C \quad (3)$$

where, $\psi_i(r) = \int_{L_{0i}} \ln|r - r_i| \frac{ds}{V_0}$, with $r = (x,y)$, and λ_i and C are determined from the following system of linear equations:

$$\begin{cases} (\mathbf{S} + \alpha \mathbf{I}) \boldsymbol{\Lambda} + \mathbf{C} \mathbf{t}_0 = \boldsymbol{\delta t} \\ \boldsymbol{\Lambda}^T \mathbf{t}_0 = \mathbf{0} \end{cases} \quad (4)$$

where $S_{ij} = \int_{L_{0i}} \int_{L_{0j}} \ln|r_i - r_j| \frac{ds_i}{V_0} \frac{ds_j}{V_0}$.

[2] The value of the regularisation parameter is chosen so that the allowed velocity range in the solution isn't less than the velocity range in the data set.

Figure 2: Tomography maps at different periods, from 10 s to 35 s. In each map the percent variation of the Group Velocity dU/U with respect to the mean velocity value calculated on the whole area (here indicated by Ref.) is plotted at the chosen period. At the bottom, the scale of the velocity percent variation is presented. In each plot the area with a low or bad path coverage is left white.

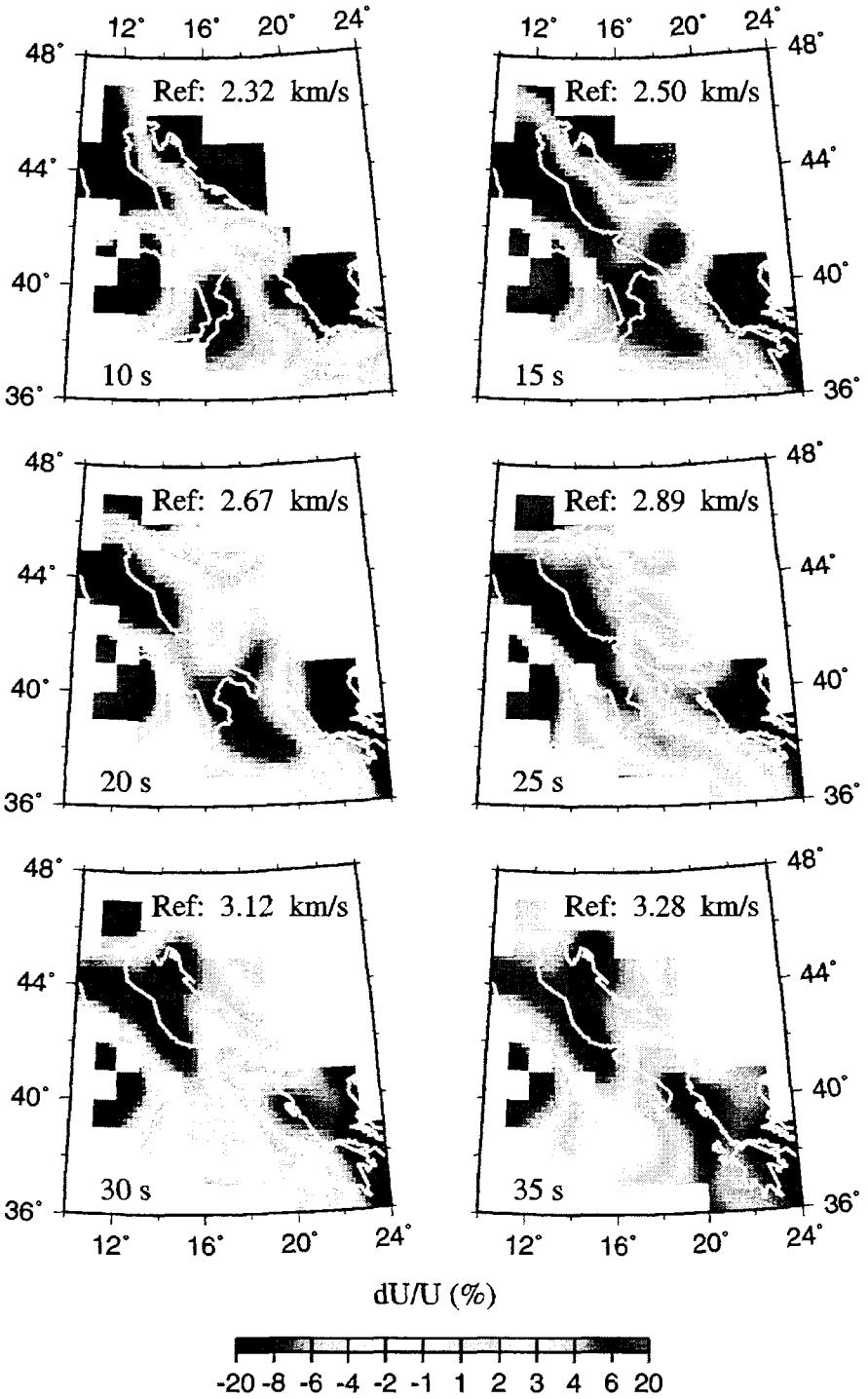

2.3 Tomography images of group velocity.

In each map of Fig.2, the percent deviation with respect to the mean group velocity U_{mean} calculated over the whole area at a fixed period, in the period range of 10-35 s, is given. The percent deviation of group velocity, at the period T and at the point (x,y), is defined as:

$$\left(\frac{dU(x,y)}{U(x,y)}\right)_T = \left(\frac{U_{mean} - U(x,y)}{U(x,y)}\right)_T .$$

The group velocity maps reveal the presence of significant lateral variations at each of the selected periods, with reliable (where the path coverage is good) percent variation smaller than 0.2. The considered period range samples the depth interval from about 5 km to about 50 km, as it can be easily seen from the values of the partial derivatives of group velocities for Rayleigh waves with respect to structural parameters (Urban et al., 1993). In general, the short periods (from 10 s to 25 s) sample the deep sediments and the upper crust, while the longer periods (from 25 s to 35s) sample the lower crust and the uppermost mantle (the lid).
Going from the shortest period to the longest one, that is from the upper crust to the upper mantle, the average group velocity progressively increases (see the Ref. velocity values at the different periods in Fig.2) and significant depth variations, due to the variety and the complexity of the tectonic and of the geological features in the studied area, can be seen.
The tomography maps at the shortest periods (10 s, 15 s and 20 s) mimic the main features of the major sedimentary deposits (Laske and Masters, 1997), in particular those in the Southern Adriatic Sea (sediment thickness bigger than about 9-10 km) and Ionian Sea (sediment thickness bigger than about 7 km).
In correspondence of the thick sedimentary layer in the southern Adriatic Sea, in the map at 10 s a negative anomaly trending NW-SE is seen. Such anomaly increases at the periods of 15 s and 20 s, but it vanishes or becomes positive at the longer periods. In the Ionian Sea, at 15 s and 20 s, the negative anomaly reproduces the NW-SE trend of the sediment thickness in that area. The strong negative anomalies, which appear at the shortest periods in the Apennines area, aren't associated to the presence of thick layers of sediments, but to the presence of low velocity crustal material, which is the result of the inherited compressional tectonics on the ongoing extensional deformation. In the maps at 30 s and 35 s, the negative anomalies in the Southern Adriatic Sea and in the Ionian Sea disappear, while in correspondence of the two mountain chains of the Apennines and the Dinarides they become more evident. Such pattern of the anomalies evidences how the orogenic process perturbs at

least the lower crust and the upper mantle, in contrast with the sedimentation process that seems to exhaust its effect in the upper crust, even when the thickness of sediments is very large.

2.4 The Resolution.

The estimation of the horizontal resolution of the 2D tomography maps at any fixed period, proposed by Yanovskaya (1997), generalises the Backus and Gilbert (1968) method and considers the direction dependence of the resolution. In fact, the density of the paths, the azimuth coverage and the average path length control the resolution of the data set. Yanovskaya (1997) defines the criterion to estimate the resolvability at a point along a fixed direction, assumed arbitrarily to coincide with the x axis: the smoothing area width, a, characterising the data resolvability can be estimated along any direction ϑ through the proper rotation of the x axis. Thus, the azimuth dependence of resolvability can be estimated at any point as $a(\vartheta) = a + b\cos(2\vartheta - 2\varphi)$. Accordingly with Yanovskaya (1997): (1) the resolvability estimation by the minimum and maximum value of the linear dimensions of the smoothing area, obtained along two mutually perpendicular directions, is equivalent to the assumption that the effective smoothing area may be represented by an ellipse with the two axes equal to $(a+b)$ and $(a-b)$, with the azimuth of the major axis being ϕ; (2) the elongation, ε, of the smoothing area is estimated by the ratio of the difference between the maximum and minimum sizes of the area to its mean size $\varepsilon = 2b/a$; (3) if the elongation, ε, in a point is a small value, that is if the traces are oriented more or less uniformly along all directions, the resolvability at that point may be characterised by the mean linear size, a, of the effective smoothing area. The values of the parameters ε and a, at the selected periods, are plotted in Fig.3 and Fig.4, respectively. Small values of the elongation $(\varepsilon < 1)$ imply that the paths are oriented more or less uniformly along all directions, while, if the elongation values are larger than the unity, the paths have a preferred orientation and the lateral resolution in this direction is quite small. The elongation values are between 0.10 and 0.75 in most of the studied area at all the considered periods; only in Puglia (SE Italy) and Greece the elongation gets close to the unity. In the central part of the studied area, the mean linear size, a, of the effective smoothing area is less or equal to 200 km at all the periods.

Figure 3: Distribution of the elongation parameter, ε, at different periods, from 10 s to 35 s.

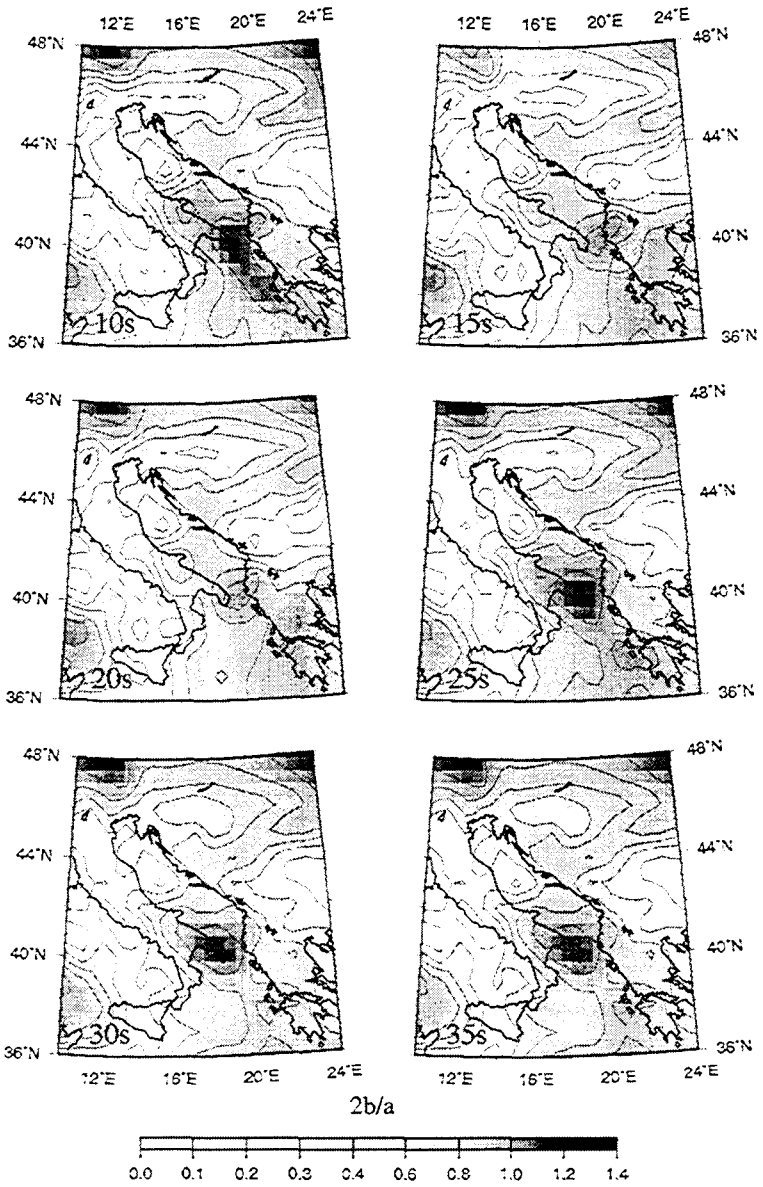

Figure 4: Distribution of the mean linear size parameter, a, at different periods, from 10 s to 35 s.

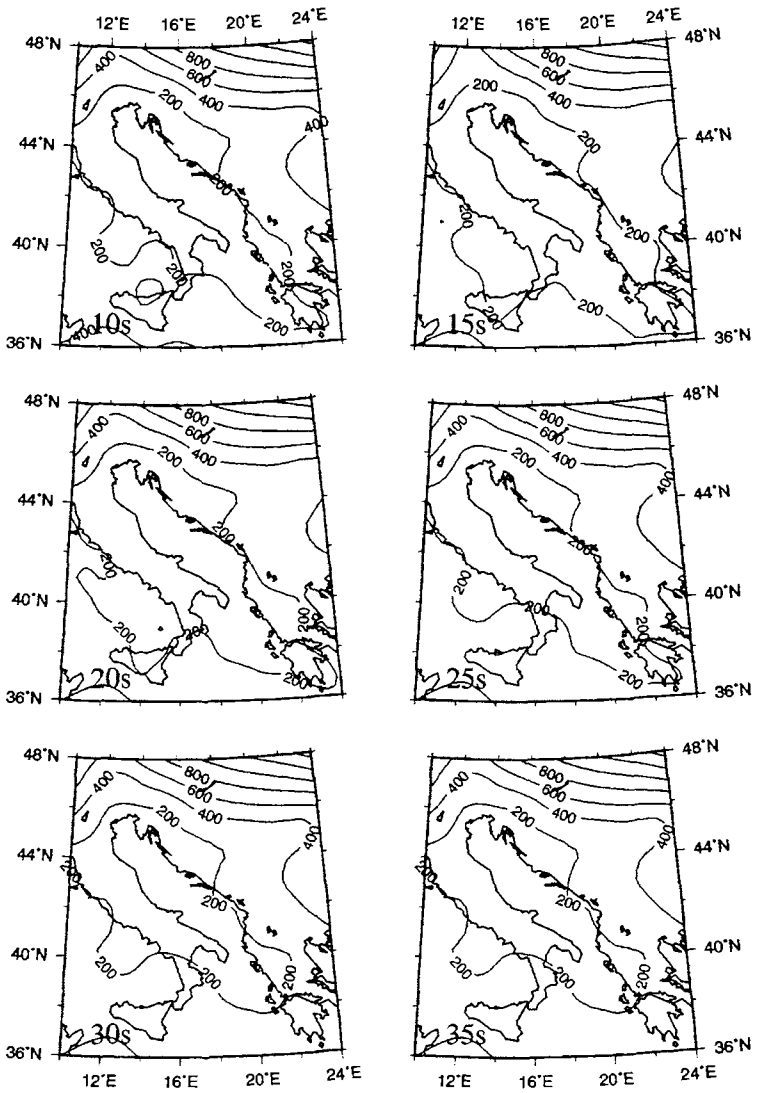

3. Regionalization of tomography maps.

The group velocity tomographic maps can be discretized with a step consistent with the value of the lateral resolution length, a. Therefore, in the central part of the study region, for each considered period, T_i, we discretize our maps along a 1°x1° grid. At each knot of the grid the group velocity value, $u_{j,n}(T_i)$, is read and thus we construct a dispersion curve. To each cell

of the grid we assign an average dispersion curve, $U_{C_j}(T_i)$, obtained by averaging, for each T_i, the values of the group velocity at the four corners (knots) of each cell[3].

The grouping of the cells is done independently from any a priori geological assumption. To regionalize the study area, the cellular dispersion curves are grouped accordingly to the following rules:

- cells with a low paths-coverage aren't considered;
- a preliminary grouping is done by the comparison of the dispersion curve of each cell with the dispersion curves of the neighbouring ones; to each group are assigned the cells with a dispersion curve that differs by less than three standard deviation, $3\sigma_{R_l}(T_i)$, at each period, from the average value, $U_{R_l}(T_i)$, calculated[4] from all the selected curves in that group (the l-group);
- the final grouping is made excluding from each group, for example from the region l, the dispersion curves that fall outside $2\sigma_{R_l}(T_i)$ from the average value $U_{R_l}(T_i)$; the excluded dispersion curves are then inserted into one of the dispersion curves group that defines one of the neighbouring regions, for example the region m, if they fall within $2\sigma_{R_m}(T_i)$ from the average value $U_{R_m}(T_i)$ of the new region.

Thus, the curves of adjacent cells are considered similar and define a region if their velocity values at each period differ, from their mean velocity values $U_{R_l}(T_i)$, by less than $2\sigma_{R_l}(T_i)$. In this way seven regions are defined with different dispersion properties and in Fig.5 the mean group velocity curves of all the 1°x1° cells are shown grouped by region. In the first seven frames, $2\sigma_{R_l}(T_i)$ bars are indicated for each region.

---

[3] Considering the group velocities $u_{j,n}$ (n=1, ..., N; with N=4) at the four knots of the j-cell, the mean group velocity for the j-cell, U_{C_j}, and its standard deviation, σ_{C_j}, at the period T_i are calculated as follows:

$$U_{C_j}(T_i)=\frac{N}{\sum_{n=1}^{N}\frac{1}{u_{j,n}(T_i)}} \quad \text{and} \quad \sigma_{C_j}(T_i)=\sqrt{\frac{\sum_{n=1}^{N}(u_{j,n}(T_i)-U_{C_j}(T_i))^2}{N}}.$$

[4] Considering the group velocities U_{C_j} (j=1, ..., M; with M the number of cells in that region) of the j-cell, the mean group velocity for the l-group, U_{R_l}, and its standard deviation, σ_{R_l}, at the period T_i are calculated as follows: $U_{R_l}(T_i)=\frac{M}{\sum_{j=1}^{M}\frac{1}{U_{C_j}(T_i)}}$ and $\sigma_{R_l}(T_i)=\sqrt{\frac{\sum_{j=1}^{M}(U_{C_j}(T_i)-U_{R_l}(T_i))^2}{M}}$.

Figure 5: In the first seven frames: grouping of the mean dispersion curves determined for each 1°x1° cell; for each region the bars of two standard deviation at each period, $2\sigma_{R_I}(T_i)$, are shown. In the last frame: the representative average curves of the seven regions are compared and the bars correspond to the estimated measurement error.

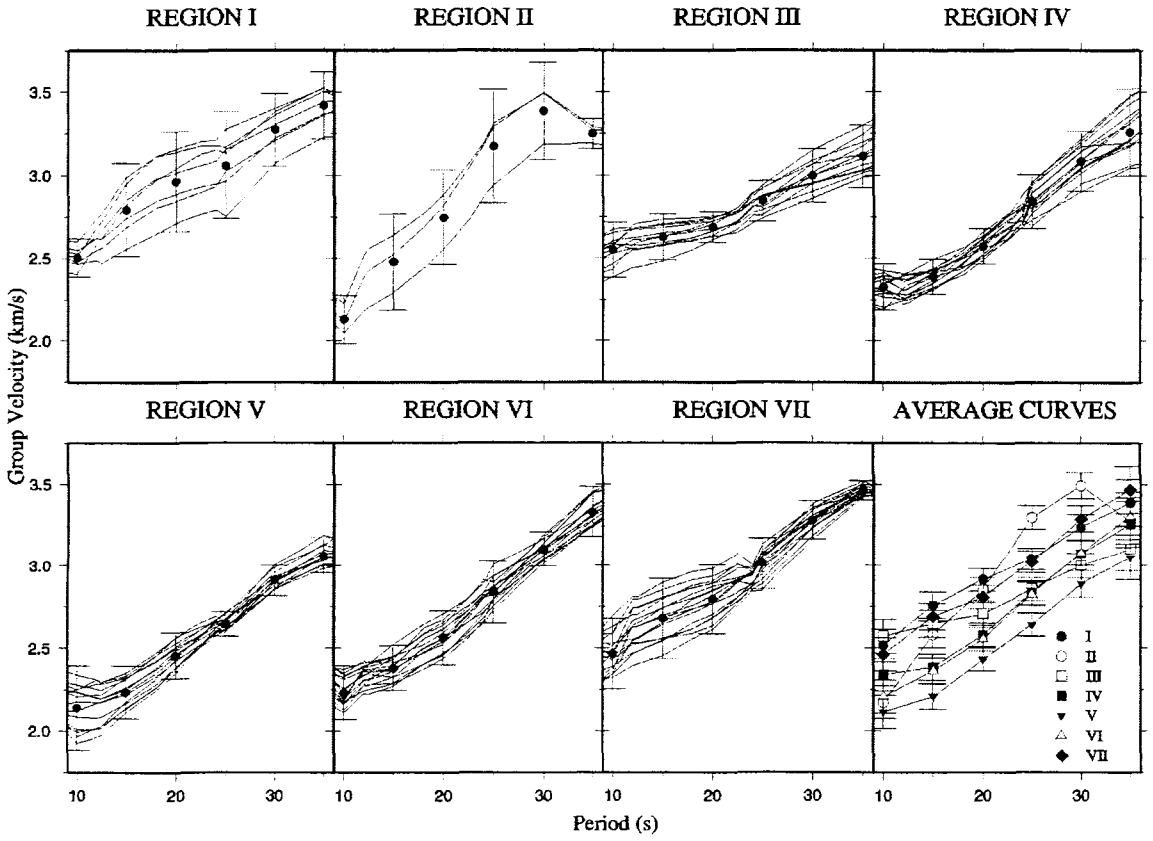

In the last frame of Fig.5 are shown the seven representative regional average curves $\hat{U}_{R_I}(T_i)$, calculated considering only the cellular curves that, on average, are within the measurement error, at each period, from the regional average value $U_{R_I}(T_i)$, calculated considering all the cells. The measurement error associated to each period of each regional average dispersion curve (error-bar in the last frame of Fig.5) is estimated from the difference in the group velocity values determined along similar paths crossing similar areas. The regional average curves $\hat{U}_{R_I}(T_i)$ and their associated measurement errors are plotted in Table C.1, in the Appendix C, for five out of the seven main regions of our regionalization. In Fig.6 it is shown the sketch of the obtained regionalization.

Figure 6: Regionalization scheme. The seven regions are identified by different hatching and each region is identified by two distinct patterns: (1) measurement-error patterns (if, at each period, the mean dispersion curve of the cell falls within the measurement error from the average curve, computed from the curves of all the cells in that region); (2) two-sigma patterns (if, at any period, the mean dispersion curve of the cell differs by more than the measurement error but less than two standard deviations from the average curve, computed from the curves of all the cells in that region).

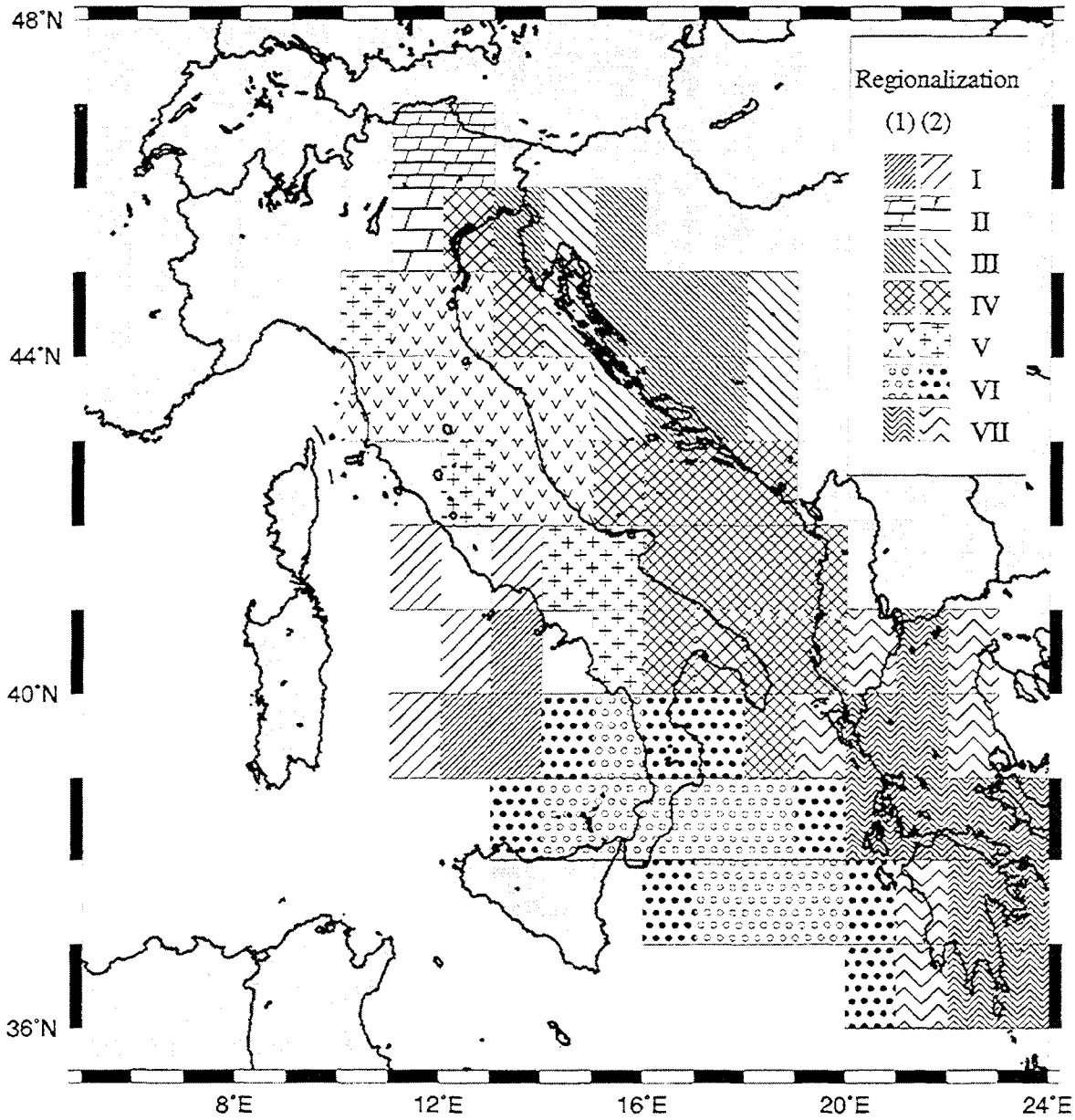

To outline each region, two distinct patterns are used: one indicates that the mean dispersion curve of the cell is, at each period, within the measurement error from the average curve in that region (measurement-error cells); the other is used where the mean dispersion curve of the cell differs, at any period, by more than the measurement error but less than two standard

deviations from the average curve (two-sigma cells). The cells without any pattern are cells with low path coverage and aren't considered in the regionalization. Taking into account the size of the used grid, seven regions can be easily correlated with the main tectonic features of the study area. Region I can be associated to most of the Southern Tyrrhenian Basin; Region II to most of the South-Eastern Alpine area; Region III to the Dinarides chain; Region IV to the Adriatic Sea and Puglia region (Italy); Region V to the Arc of the Northern Apennines and to the Southern Apennines; Region VI to the Northern part of the Ionian Sea, the Calabrian Arc and the South-Easternmost part of the Tyrrhenian Sea; Region VII to the continental part of Greece.

4. Regionalization and structural sketch.

The seven main regions can grossly be associated with Dinarides, Northern and Southern Apennines, South-eastern Alps, Adria, Southern Tyrrhenian Basin, Calabrian Arc and Greece (Fig.7).

The Northern Adriatic Sea has dispersion properties not distinguishable from those of the Southern Adriatic but a clear evidence of continuity between the two zones is missing. Thus our data show a possible extension towards N-W of Adria and its contact with the Southern-Eastern Alps (Region II), as it is in the model of Meletti et al. (2000).

To the South, the extension of Region IV is in agreement with the delineation of the Adria-Southern Apennines inactive converging plate margin (a compression front), of the Adria-Calabrian Arc and the Adria-Dinarides active fronts. The border between regions VI and VII follows quite well the Hellenic trench, at the contact between the Ionian and the Greek lithosphere.

In the zonation, the margin between Region VI and Region I, which are respectively identified as Calabrian Arc and Southern Tyrrhenian Basin in the model of Meletti et al. (2000), well corresponds to the Wadati-Benioff zone (associated to the subduction towards NW of the Ionian lithosphere). The measurement-error cells of Region I may be connected with the shallow magma sources of the Magnaghi-Vavilov and Marsili submarine seamounts in the Southern Tyrrhenian Basin.

Figure 7: The regionalization scheme is superimposed to the structural sketch (the grey lines) of Meletti et al. (2000). The seven regions, defined by surface-wave tomography, may be associated to the main features of the model: Southern Tyrrhenian Basin (Region I), Southern-Eastern Alps (Region II), Dinarides (Region III), Adria (Region IV), Northern Apenninic Arc and Southern Apennines (Region V), Calabrian Arc (Region VI), Greece (Region VII).

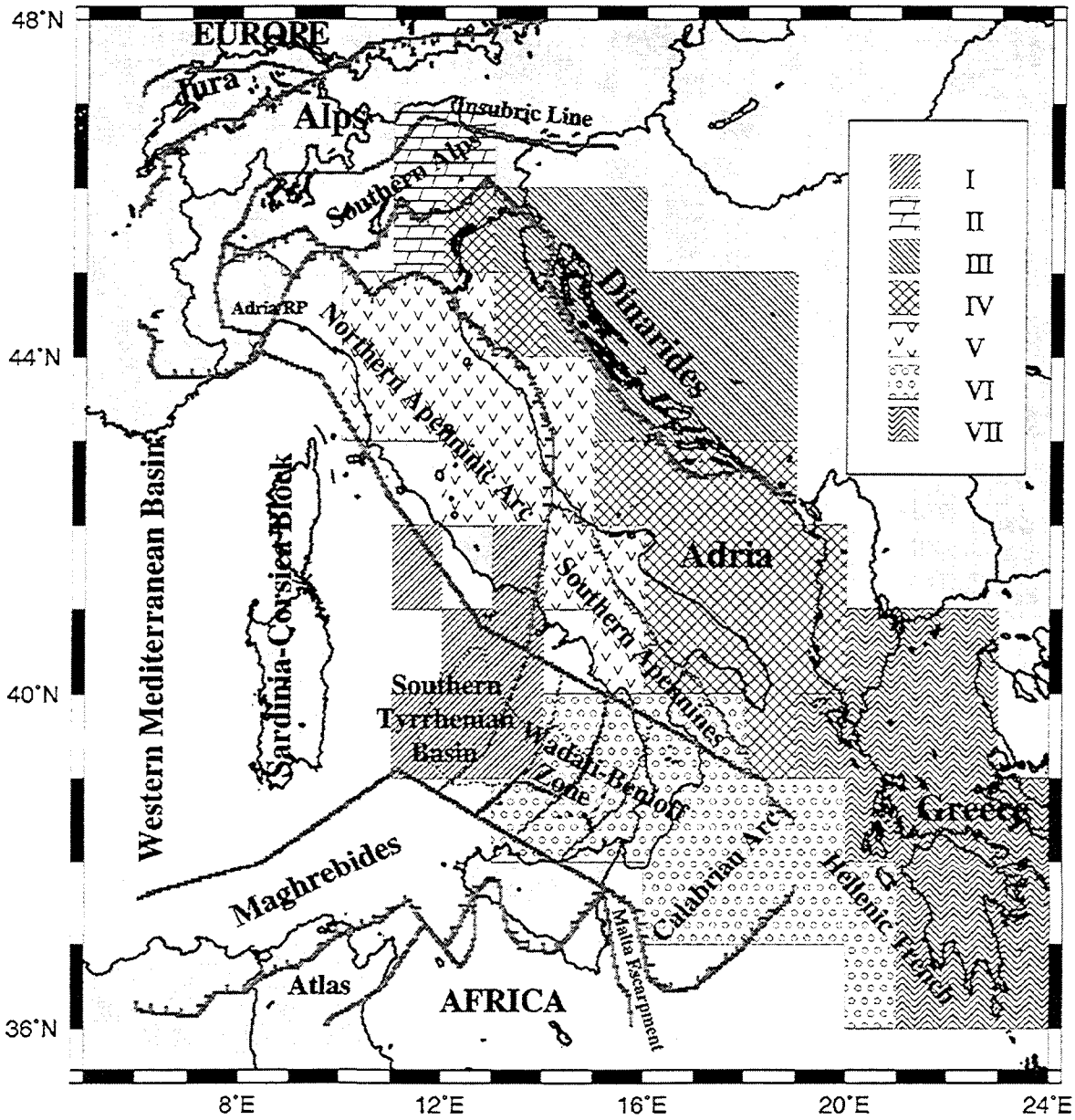

5. Average lithospheric models.

From Panza (1981) experiments on the resolving power of dispersion measurements with respect to structural parameters in the crust and in the upper mantle, Rayleigh wave group velocities lead, in general, to a better resolution as compared with phase velocities. The results of the inversion experiments (Panza, 1981) clearly indicate that the sub-Moho S-wave velocity can be determined with a rather good accuracy using indifferently phase or group velocity data, while crustal parameters are better resolved by group velocities.

The average group and phase velocity curves (see Table C.1 in the Appendix C), representative of the measurement-error area of a region, are used to perform the non-linear inversion with the hedgehog method (Valyus et al., 1969; Valyus, 1972; Knopoff, 1972) to define average models of the shear wave velocity distribution within the crust and the upper mantle. The inversion method used represents an optimised Monte Carlo search to find velocity-depth distributions consistent with the experimental observations. Following this procedure, in the elastic approximation, the structure is modelled as a stack of N homogeneous isotropic layers, each one defined by compressional and shear wave velocities, thickness and density. The structure is parametrizated (see Tables C.2 and C.3 in the Appendix C) and each parameter can be fixed (during the inversion the parameter is held constant accordingly to independent geophysical evidences), independent (the variable parameters that can be well resolved by the data) or dependent (the parameter has a fixed relationship with an independent parameter). For each structural model, phase and group velocity curves are computed and if, at each period, the difference, $\hat{d}_i$, between the computed and the experimental values (obtained from tomography and regionalization), is less than the error (for phase velocity the error is been chosen following Caputo et al., 1976; for group velocity the considered error is the measurement error, that is the error-bar shown in the last frame of Fig.5), and if the r.m.s. of the differences is less than a chosen fraction (usually about 60%) of the average between the error values, the model is accepted (Panza, 1981). The problem is not unique and in such a way a set of accepted structures is defined. For the choice of the parametrization and of the ranges of variability of the velocity and thickness parameters, we take into account the resolving power of the data (Knopoff and Panza, 1977; Panza 1981) and relevant petrological information (e.g. Ahrens, 1973; Bottinga and Steinmetz, 1979; Graham, 1970; Della Vedova et al., 1991; Ringwood, 1966) that allow us to

fix upper (4.85 km/s) and lower (4.0 km/s) limits to the upper mantle S-wave velocity (see Table C.2 in the Appendix C).

Figure 8: The solutions (the structural model described by the S-wave velocity as function of the depth), obtained from the non-linear inversion of the representative average dispersion curves, for five out of the seven main regions. For each region, a representative structural solution is shown and the Moho is marked with M. The shaded areas represent the portion of parameters space explored during the inversion. In each smaller frame, the group velocity values corresponding to the model (white circles) are compared with the experimental values (black triangles), and the measurement-error bars (the same of the last frame of Fig.5) are given.

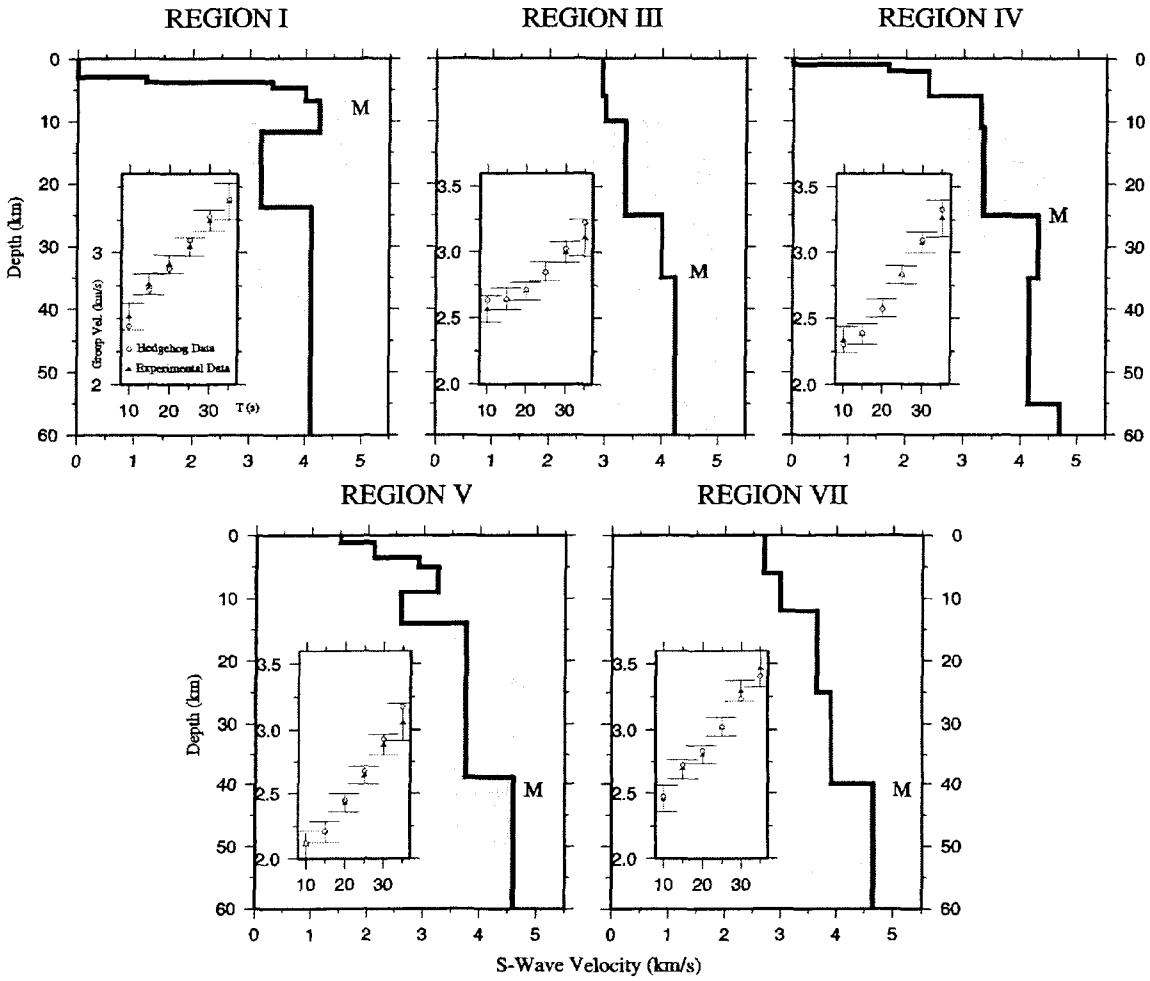

The available interpretations of the seismic profiles that cross most of the peninsula and adjacent seas and other information available from literature (Bally et al., 1986; Barchi et al., 1998; Finetti and Del Ben, 1986; Calcagnile et al., 1982; Mantovani et al., 1985; Bondar et al., 1995; Zivcic et al., 2000; Catalano et al., 2001), are used to fix the thickness and the P-wave velocity of the uppermost crustal layers, assumed to be formed by Poissonian solids, while the density is estimated from the Nafe-Drake relation (e.g. Fowler, 1995) that connects

seismic velocities and density. The same relation between P and S wave velocities and density have been used for all the dependent parameters in the inversion.

The solutions that we have chosen as representative models for five out of the seven main regions of our regionalization are plotted in Fig.8. As a matter of fact, Region II is barely resolved by the considered data and in Region VI coexist many different tectonic features for which a single set of average models has only a mathematical meaning and cannot have any geological significance.

In the Southern Tyrrhenian Basin (Region I) the Moho is very shallow (less than 10 km deep) and the lid thickness is of about 10 km. These features are in agreement with what we already know about the basin, that is characterised by a thin continental crust, whose thickness reduces progressively going from the borders towards the basin centre (Pepe et al., 2000), where the crust is oceanic.

Below the lid, with an S-wave velocity of about 4.25 km/s, there is a very well developed low velocity channel about 12 km thick, centred at a depth of about 18 km. At greater depth, the velocity is around 4.1 km/s. In the thin and very strong channel the S-wave velocity can be as low as 3.2 km/s, therefore the partial melting there can be as high as 10% (Bottinga and Steinmetz, 1979). This high percentage of partial melting, that seems to be a regional feature, is well compatible with the presence of shallow anomalous mantle materials (Trua et al., 2001) in correspondence of the huge volcanic structures like the Vavilov-Magnaghi and Marsili seamounts.

The Moho depth in Region III (the Dinarides chain) is at about 35 km (in agreement with the EurID data of Du et al., 1998) and in the crust S-wave velocity progressively increases with increasing depth. The lid is characterised by an S-wave velocity gradient, starting at about 4.25 km/s.

In Region IV (the Adriatic Sea) the crust has a continental character: the sharp Moho is at a depth of about 25 km, and the S-wave velocity just below the crust is about 4.3 km/s. The lid is characterised by a gradient with the maximum velocity value at about 4.7 km/s.

In the Apenninic area of Region V, the Moho is at a depth of about 40 km and its lid has an S-wave velocity around 4.6 km/s. The high S-wave velocity at depths exceeding 50 km confirm the presence of lithospheric roots (Calcagnile and Panza, 1981; Du et al., 1998) marked by rare, but now regularly recorded, seismic activity (Amato et al., 1997; Cattaneo et al., 1999).

The continental part of Greece in Region VII presents a sharp Moho at about 40 km of depth and the lid velocity at about 4.65 km/s.

6. Discussion and conclusions.

From the tomography maps constructed from single path group velocity measurements of Rayleigh waves, we can distinguish areas with different dispersion properties, due to important lateral variations in the physical properties of the crust and of the upper mantle.
We define seven different regions, each characterised by a distinctive mean group dispersion curve, whose geometry mimics well enough the structural sketch of the studied area as proposed by Meletti et al. (2000).
The non-linear inversion of the distinctive dispersion data of selected regions allows us to define average models of the shear wave velocity in the crust and the upper mantle, that represent a refinement of our knowledge about the structure of the study area, well in agreement with the existing models (e.g. Du et al., 1998).
In the Southern Tyrrhenian Basin, the crust is oceanic and a very well developed and shallow low velocity channel is present in the upper mantle. Such a structural model is compatible with the presence of the huge volcanic structures like the Vavilov-Magnaghi and Marsili seamounts.

Acknowledgments.

We wish to thank the Working Group on Active Faulting and Seismic Hazard in Attiki of the Environment and Climate Project and in particular we are grateful to E. Karagianni for the Greek data provided (MIL, KAP and LIT stations), J. Bajc and M. Zivcic of the Geophysical Survey of Slovenia for the Slovenian data provided (LJU, BISS and CEY stations), C. Eva, P. Augliera and D. Spallarossa of the Department of Earth Sciences of Genova for the data recorded by GENL station, the Department of Earth Sciences of Trieste and OGS for the data recorded by TRI station. We are grateful to T.B. Yanovskaya for the very useful advices on the tomography method and to C. Doglioni for the very fruitful discussion about the geological aspects. This work has been supported by the projects: CNRC007AF8, MURST prot. 9904261312_006 (1999), MURST prot. MM04158184_002 (2000).

Appendix A. Group Velocity Data.

In the following Tables (A.1, A.2, A.3) are plotted: the Data, Origin Time, Latitude and Longitude of the Events; Code, Latitude and Longitude of the Recorder Stations; the epicenter-station distance (km); the values of the group velocity, calculated through interpolation at different periods in the period range of 10s-35s.

Table A.1: List of events processed by FTAN. Data are provided by: Active Faulting and Seismic Hazard in Attiki, Environment and Climate Project (MIL, KAP and LIT stations); Geophysical Survey of Slovenia (LJU, BISS and CEY stations); Dept. of Earth Sciences of Genova (GENL station); ORFEUS (AQU station); Dept. of Earth Sciences of Trieste and OGS (TRI station).

Date	O. Time	Event		Station			km	Group Velocity (km/s) at different Periods (10s-35s)					
Y.-J.D.-G.D.	H-m-s	Lat.	Long.	Code	Lat.	Long.	Ev.-St.	10s	15s	20s	25s	30s	35s
1996 254 10/09	05 09 25.860	45.4360	16.2180	BISS	46.6478	15.1272	158.96	2.46796	2.49590	2.59176	2.69269	2.79758	-
1996 289 15/10	09 55 59.630	44.7920	10.7800	BISS	46.6478	15.1272	396.25	2.35549	2.42200	2.47009	2.58355	-	-
1997 269 26/09	00 33 12.250	43.0480	12.8790	BISS	46.6478	15.1272	437.69	2.48471	2.54381	2.57559	2.66787	2.84587	3.02997
1997 276 03/10	08 55 21.580	43.0750	12.7940	BISS	46.6478	15.1272	437.72	2.58073	2.56028	2.59093	2.69782	2.89794	3.11014
1997 027 27/01	00 46 16.810	45.2240	16.1940	CEY	45.7388	14.4267	149.54	2.46620	2.37053	2.44387	2.53474	2.61755	2.69078
1997 298 25/10	03 08 06.130	42.8380	13.0090	CEY	45.7388	14.4267	341.6	2.40982	2.51062	2.56253	2.66032	2.78106	-
1997 358 24/12	17 53 08.460	44.0920	10.5510	CEY	45.7388	14.4267	356.52	2.15790	2.21960	2.27942	2.37146	2.55562	2.79739
1996 230 17/08	15 54 07.650	43.9690	15.4100	LJU	46.0438	14.5274	240.84	3.14127	3.66442	3.94278	3.99550	-	-
1996 289 15/10	09 55 59.630	44.7920	10.7800	LJU	46.0438	14.5274	324.59	2.35197	2.40232	2.44258	-	-	-
1996 289 15/10	12 18 24.140	44.7850	10.7280	LJU	46.0438	14.5274	328.62	2.39974	2.40521	2.36595	-	-	-
1997 269 26/09	00 33 12.250	43.0480	12.8790	LJU	46.0438	14.5274	357.72	2.37029	2.45984	2.50582	2.63480	2.79706	2.89560
1997 275 02/10	19 38 02.240	43.6380	12.1350	LJU	46.0438	14.5274	327.46	2.47316	2.44065	2.36251	2.27073	2.21750	-
1997 276 03/10	08 55 21.580	43.0750	12.7940	LJU	46.0438	14.5274	357.47	2.35525	2.51914	2.58013	2.76058	2.99280	3.14441
1997 287 14/10	15 23 10.210	42.9620	12.8920	LJU	46.0438	14.5274	366.29	2.38172	2.47965	2.53398	-		
1990 150 30/05	10 40 06.140	45.8410	26.6680	AQU	42.3540	13.4050	1128.83	2.32356	2.39933	2.62647	3.14672	3.39552	3.59661
1990 151 31/05	00 17 47.850	45.8110	26.7690	AQU	42.3540	13.4050	1135.53	2.25250	2.30795	2.53935	2.88641	3.34769	3.65418
1990 331 27/11	04 37 58.500	43.8530	16.6330	AQU	42.3540	13.4050	311.06	2.17878	2.38247	2.46646	2.60759	2.77760	2.89207
1990 331 27/11	04 51 36.400	43.8950	16.6410	AQU	42.3540	13.4050	314.05	2.19118	2.39251	2.44628	2.51956	2.60499	2.65057
1991 199 18/07	11 56 30.600	44.8880	22.4070	AQU	42.3540	13.4050	778.69	2.53086	2.59752	2.65411	2.86096	3.11262	3.32940
1991 200 19/07	01 27 32.000	45.3120	21.0530	AQU	42.3540	13.4050	697.01	2.39391	2.55161	2.63876	2.80946	3.00161	3.16886
1991 336 02/12	08 49 40.200	45.4980	21.1150	AQU	42.3540	13.4050	710.45	2.39054	2.55687	2.65288	2.80277	2.98062	3.16425
1992 080 20/03	05 37 23.900	36.6620	24.5200	AQU	42.3540	13.4050	1144.43	2.41062	2.42531	2.55232	2.87388	3.15284	3.18042
1992 121 30/04	11 44 38.900	35.0590	26.6550	AQU	42.3540	13.4050	1405.9	2.13261	2.38764	2.64815	2.88037	3.19858	3.44095
1992 151 30/05	18 55 40.100	38.0790	21.4440	AQU	42.3540	13.4050	832.23	2.30670	2.46203	2.66373	2.97642	3.18715	3.31938
1992 173 21/06	18 59 05.100	39.1370	19.8070	AQU	42.3540	13.4050	647.76	2.71741	2.73360	2.73843	2.70423	2.55999	2.43331
1992 205 23/07	20 12 42.500	39.8470	24.3900	AQU	42.3540	13.4050	963.09	2.44611	2.68801	3.19733	-	-	-
1992 273 29/09	15 04 08.100	34.4780	14.4830	AQU	42.3540	13.4050	879.3	2.45106	2.51767	2.73132	2.91351	3.15064	3.36446
1992 311 06/11	19 08 09.200	38.1600	26.9980	AQU	42.3540	13.4050	1244.84	2.44695	2.59645	2.68775	2.84122	3.11535	3.35363
1992 323 18/11	21 10 41.400	38.3070	22.4520	AQU	42.3540	13.4050	889.79	2.49268	2.57856	2.75814	2.95956	3.13088	3.27808
1992 326 21/11	05 07 21.700	35.9160	22.4910	AQU	42.3540	13.4050	1060.9	2.00885	2.05696	2.14977	2.43326	3.03015	3.44740
1992 326 21/11	12 55 49.000	45.6710	26.6560	AQU	42.3540	13.4050	1123.07	2.14531	2.24390	2.31503	2.52732	2.84723	3.11172
1993 035 04/02	02 22 57.170	38.2420	22.6680	AQU	42.3540	13.4050	909.57	2.63225	2.63432	2.77684	2.94202	3.09044	3.22548
1993 064 05/03	06 55 08.630	37.1780	21.5050	AQU	42.3540	13.4050	900.35	2.60569	2.70034	2.76064	2.79939	2.83262	3.06192
1993 077 18/03	15 47 00.420	38.3400	22.1550	AQU	42.3540	13.4050	866.11	2.81428	2.81406	2.84574	2.92149	3.08624	3.29870
1993 085 26/03	11 58 15.170	37.5890	21.3910	AQU	42.3540	13.4050	862.68	2.62607	2.78079	2.97137	3.13975	3.23626	3.25948

1993 149 29/05	08 43 11.600	45.5610	15.2070	AQU	42.3540	13.4050	384.54	1.79030	1.84850	1.87405	1.92678	2.07526	2.20656
1993 152 01/06	09 45 29.500	34.3520	26.1840	AQU	42.3540	13.4050	1424.38	2.31603	2.38512	2.56520	2.80737	2.97987	3.14357
1993 152 01/06	19 51 10.900	46.1660	16.4670	AQU	42.3540	13.4050	488.99	2.20651	2.42940	2.51937	2.67734	2.89112	3.09352
1993 156 05/06	19 16 16.800	43.1210	12.6780	AQU	42.3540	13.4050	103.94	2.74828	2.57983	2.43303	2.36296	2.36786	2.42028
1993 164 13/06	23 26 40.400	39.3630	20.4950	AQU	42.3540	13.4050	683.54	2.80624	2.76949	2.85291	3.25531	3.67762	3.81903
1993 274 01/10	03 59 33.000	36.6370	23.9670	AQU	42.3540	13.4050	1106.92	2.47429	2.50750	2.60942	2.88375	3.12366	3.26448
1993 358 24/12	21 53 19.800	40.1580	19.8150	AQU	42.3540	13.4050	589.77	2.57311	2.58957	2.62777	2.75506	2.97226	3.18487
1996 249 05/09	20 44 09.290	42.8030	17.9360	GENL	44.4050	8.96900	745.1	2.46523	2.57506	2.66346	2.80028	3.00286	3.22991
1996 261 17/09	13 45 22.880	42.8660	17.8200	GENL	44.4050	8.96900	734.01	2.24705	2.30645	2.38519	2.51059	2.63059	2.68139
1996 289 15/10	10 19 43.670	44.7540	10.7430	GENL	44.4050	8.96900	146.13	2.39710	2.44159	2.42156	2.38978	-	-
1996 289 15/10	12 18 24.140	44.7850	10.7280	GENL	44.4050	8.96900	145.9	2.26281	2.31531	2.24984	2.15244	2.11779	2.13579
1996 294 20/10	19 06 55.350	42.6010	13.2780	GENL	44.4050	8.96900	401.92	2.36352	2.34336	2.39216	2.49187	2.56333	2.60243
1997 084 25/03	00 46 13.830	36.9300	16.0300	KAP	35.5500	27.1700	1012.4	2.57509	2.68203	2.92451	-	-	-
1997 084 25/03	00 46 13.830	36.9300	16.0300	MIL	36.6800	24.4400	750.76	2.31528	2.69041	3.11592	3.28037	-	-
1997 160 09/06	14 10 58.240	38.7160	16.3990	LIT	40.1000	22.4900	546.5	2.64174	2.73548	2.91428	3.04770	3.12965	3.20387
1997 186 05/07	20 18 14.790	38.0860	17.1330	MIL	36.6800	24.4400	665.48	2.28927	2.27731	2.31862	2.33634	-	-
1995 198 17/07	23 18 15.750	40.1920	21.5320	AQU	42.3540	13.4050	721.67	2.32387	2.52477	2.57557	2.55704	-	-
1998 085 26/03	16 26 11.510	43.2550	12.9690	BGY	44.8026	20.5158	628.7	2.43764	2.45836	2.60837	2.81085	2.96429	3.06177
1996 249 05/09	20 44 09.290	42.8030	17.9360	TRI	45.7090	13.7640	463	2.80485	2.74455	2.77120	2.84932	2.96951	3.08647
1996 249 05/09	21 43 31.140	42.8260	17.8450	TRI	45.7090	13.7640	456.8	2.80048	2.74607	2.76720	2.82565	2.95096	3.12546
1996 253 09/09	15 57 05.140	42.7740	17.8730	TRI	45.7090	13.7640	462.5	2.80054	2.76043	2.80044	2.89137	3.02245	3.15763
1996 254 10/09	05 09 25.860	45.4360	16.2180	TRI	45.7090	13.7640	193.9	2.58290	2.45187	2.42910	2.60458	2.83194	2.99959
1996 277 03/10	22 41 00.520	46.2300	15.0810	TRI	45.7090	13.7640	117	2.81224	2.82028	2.84393	2.88247	2.93845	2.99272
1996 289 15/10	09 55 59.630	44.7920	10.7800	TRI	45.7090	13.7640	255.4	2.13051	2.25826	2.40821	2.60840	2.79902	2.93670
1996 294 20/10	15 00 02.690	42.8080	17.8150	TRI	45.7090	13.7640	456.5	2.81068	2.78179	2.87163	3.01538	3.17026	3.29908
1996 356 21/12	08 46 01.040	40.0390	13.0230	TRI	45.7090	13.7640	632.7	3.30617	3.66059	3.54466	3.43535	3.49316	3.61652
1997 019 19/01	19 42 38.420	40.8170	19.6650	TRI	45.7090	13.7640	724	2.45354	2.43607	2.47874	2.64769	2.86049	3.08213
1997 136 16/05	07 00 48.370	41.0510	20.1700	TRI	45.7090	13.7640	732	2.27861	2.39221	2.55700	2.73872	2.93733	3.15008
1997 146 26/05	23 38 55.430	43.2420	17.5430	TRI	45.7090	13.7640	406	2.89465	2.95515	3.07050	3.20969	-	-
1997 156 05/06	20 22 56.960	47.3440	10.6920	TRI	45.7090	13.7640	297.6	2.97981	3.05956	3.19428	3.34878	3.44898	3.51837
1997 208 27/07	10 07 52.550	35.5820	21.0640	TRI	45.7090	13.7640	1281.6	2.64703	2.69490	2.79466	3.02879	3.27643	3.43929
1997 223 11/08	06 40 11.340	44.6620	10.0140	TRI	45.7090	13.7640	316	2.16264	2.38944	2.51171	2.69889	2.90300	3.06692
1997 262 19/09	12 00 27.008	40.0200	21.3260	TRI	45.7090	13.7640	883.1	2.79202	2.81463	2.84108	2.86688	2.93759	3.05037
1997 269 26/09	00 33 12.250	43.0480	12.8790	TRI	45.7090	13.7640	304	2.27022	2.44328	2.51949	2.69576	2.86500	2.98171
1997 269 26/09	04 44 36.860	42.5540	13.3780	TRI	45.7090	13.7640	351	2.65000	2.74727	2.85778	3.04033	3.24608	3.41329
1997 269 26/09	09 40 26.330	43.0840	12.8120	TRI	45.7090	13.7640	301	2.27896	2.43974	2.51282	2.66301	2.84572	2.99321
1997 275 02/10	21 38 42.520	43.6400	12.1230	TRI	45.7090	13.7640	264	2.43232	2.39622	2.48134	2.66598	2.83180	2.93934
1997 276 03/10	08 55 21.580	43.0750	12.7940	TRI	45.7090	13.7640	302	2.29162	2.45782	2.55211	2.72616	2.92022	3.05713
1997 279 06/10	23 24 52.580	43.0450	12.8350	TRI	45.7090	13.7640	305	2.24168	2.45009	2.60491	2.75477	2.88710	2.98404
1997 286 13/10	13 39 37.490	36.3790	22.0710	TRI	45.7090	13.7640	1248	2.51287	2.51638	2.63538	2.95273	3.19402	3.47471
1997 287 14/10	15 23 10.210	42.9620	12.8920	TRI	45.7090	13.7640	313	2.29055	2.45083	2.53894	2.69502	2.89834	3.06982
1997 298 25/10	03 08 06.130	42.8380	13.0090	TRI	45.7090	13.7640	324	2.37694	2.53496	2.63535	2.78494	3.00001	3.24526
1997 309 05/11	21 10 28.680	38.4380	22.2840	TRI	45.7090	13.7640	1070	2.76227	2.90753	3.00795	3.07523	3.13487	3.20726
1997 316 12/11	16 26 58.710	39.3420	20.2340	TRI	45.7090	13.7640	884.12	2.04469	2.20111	2.37523	2.73694	3.32272	3.70514
1997 317 13/11	00 48 45.770	43.3120	20.3510	TRI	45.7090	13.7640	587.3	2.85074	2.75961	2.63864	2.65325	2.87950	3.18195
1997 322 18/11	15 23 31.830	37.3530	21.1720	TRI	45.7090	13.7640	1114	2.13530	2.22224	2.38926	2.87832	3.32850	3.60990
1997 358 24/12	17 53 08.460	44.0920	10.5510	TRI	45.7090	13.7640	311	2.10310	2.20045	2.32615	2.52479	-	-
1998 026 26/01	23 17 12.899	42.3660	16.2970	TRI	45.7090	13.7640	423.26	2.70669	2.65907	2.66003	2.81959	3.11505	3.36501
1998 060 01/03	07 22 41.810	43.3580	17.6310	TRI	45.7090	13.7640	403	2.85404	2.86086	2.85834	2.88429	2.95170	3.02264
1998 085 26/03	16 26 11.510	43.2550	12.9690	TRI	45.7090	13.7640	280	2.29096	2.32133	2.43504	2.61334	2.80993	2.97807
1998 093 03/04	07 26 36.630	43.1640	12.7010	TRI	45.7090	13.7640	295	2.44693	2.50894	2.59800	2.74474	2.92143	3.04828
1998 095 05/04	15 52 20.070	43.1850	12.7190	TRI	45.7090	13.7640	292	2.31738	2.50185	2.59602	2.74557	2.90029	3.01894
1998 097 07/04	21 36 54.780	41.1110	15.8100	TRI	45.7090	13.7640	536.99	2.60293	2.64209	2.78757	3.00114	3.21546	3.36567
1998 119 29/04	03 30 39.340	36.1380	21.9400	TRI	45.7090	13.7640	1265	2.46323	2.51703	2.63452	2.74106	2.90664	3.07711
1998 120 30/04	10 59 01.400	36.0420	21.9780	TRI	45.7090	13.7640	1276	2.38472	2.49231	2.66435	2.78156	2.93509	3.07406

1998 121 01/05	04 00 13.020	37.4940	20.7400	TRI	45.7090	13.7640	1081	2.56546	2.59353	2.65147	3.10932	3.44355	3.59722
1998 129 09/05	13 06 13.440	40.9860	20.0010	TRI	45.7090	13.7640	729	2.00916	2.16947	2.32818	2.44582	2.56453	2.69975
1998 132 12/05	15 18 03.150	46.1720	16.6070	TRI	45.7090	13.7640	226	2.71147	2.74708	2.93688	3.06707	3.02463	2.92270
1998 140 20/05	11 07 41.370	43.0810	10.7040	TRI	45.7090	13.7640	380	1.99560	2.34964	2.61976	2.86533	3.11917	3.34802
1998 153 02/06	18 02 56.110	46.0690	16.9930	TRI	45.7090	13.7640	253	2.70631	2.78339	2.92484	3.06342	-	-
1998 153 02/06	23 11 22.560	43.1750	12.7580	TRI	45.7090	13.7640	292	2.33960	2.50184	2.61556	2.78468	2.93161	3.02389
1998 154 03/06	18 00 42.390	45.7200	10.8370	TRI	45.7090	13.7640	227.89	2.71825	2.71302	2.72504	2.80834	2.89572	2.97784
1998 171 20/06	02 25 58.060	38.4250	12.6710	TRI	45.7090	13.7640	814	2.67955	2.81230	2.89186	3.04849	3.22029	3.35789
1998 176 25/06	00 32 52.740	42.9740	12.7520	TRI	45.7090	13.7640	314	2.41952	2.58035	2.67820	2.85844	3.06593	3.21654
1998 176 25/06	00 44 43.590	43.0890	12.6010	TRI	45.7090	13.7640	305	2.39255	2.56574	2.62618	2.74885	2.88864	2.98855
1998 273 30/09	23 42 54.210	41.9250	20.3900	TRI	45.7090	13.7640	678	2.73290	2.67562	2.62252	2.65334	2.79953	3.01920
1998 279 06/10	12 27 41.970	37.2470	21.1070	TRI	45.7090	13.7640	1121	2.52347	2.59660	2.57069	2.57585	2.70991	3.10097
1999 017 17/01	19 32 12.590	39.0680	17.7940	TRI	45.7090	13.7640	808.61	1.99085	2.20725	2.42750	2.52762	2.69928	2.92932
1999 018 18/01	20 11 18.500	41.7790	15.8840	TRI	45.7090	13.7640	468.81	2.36788	2.58245	2.78183	-	-	-
1999 025 25/01	22 45 57.660	44.0210	11.9220	TRI	45.7090	13.7640	237.43	2.39982	2.40388	2.59080	2.94500	3.23070	3.38191
1999 095 05/04	07 51 56.970	40.7670	15.3530	TRI	45.7090	13.7640	563.97	2.45529	2.46098	2.43617	2.41916	2.41462	2.41932
1999 120 30/04	03 30 37.820	44.1780	19.9980	TRI	45.7090	13.7640	520.43	2.80528	2.78076	2.85143	2.95845	2.84130	2.74377
1999 120 30/04	07 41 01.580	44.2010	20.0490	TRI	45.7090	13.7640	523.32	2.80341	2.84190	3.00119	3.24703	3.46253	3.61154
1999 162 11/06	07 50 14.360	37.6190	21.1280	TRI	45.7090	13.7640	1086.8	2.59090	2.67167	2.86274	2.94685	2.94721	3.06349

Table A.2: List of the events collected from Calcagnile et al. (1982) and integrated by data collected from Farrugia et al (1981) (the events with the asterisk).

Date	O. Time	Event		Station			Km	Group Velocity (km/s) at different Periods (10s-35s)					
Y.-J.D.-G.D.	H-m-s	Lat.	Long.	Code	Lat.	Long.	Ev.-St.	10s	15s	20s	25s	30s	35s
1974 021 21/01	20 11 57.6	38.9000	15.4000	BAI	40.8770	17.2030	268.2	-	2.29156	2.44315	-	-	-
1974 029 29/01	13 11 02.0	37.6000	14.9000	BAI	40.8770	17.2030	414.6	-	2.75719	2.88389	-	-	-
1974 029 29/01	15 12 44.8	38.3000	22.0000	BAI	40.8770	17.2030	501.6	-	2.75656	2.82833	-	-	-
1974 081 22/03	17 02 20.0	40.7000	20.5000	BAI	40.8770	17.2030	279.0	-	2.26187	2.41222	-	-	-
1974 097 07/04	14 22 47.7	34.7000	24.7000	BAI(*)	40.8770	17.2030	951.2	2.58000	2.56251	2.57557	2.90000	-	-
1974 155 04/06	14 19 06.8	38.9000	17.8000	BAI	40.8770	17.2030	225.4	-	1.87813	1.84185	-	-	-
1974 180 29/06	01 06 58.0	36.7000	5.20000	BAI	40.8770	17.2030	1140.0	-	2.83375	2.90370	-	-	-
1974 190 09/07	02 32 15.4	36.4000	28.5000	BAI	40.8770	17.2030	1100.8	-	2.73625	2.78296	-	-	-
1974 327 23/11	07 52 28.9	39.9000	18.9000	BAI	40.8770	17.2030	180.3	-	2.29313	2.28185	-	-	-
1974 327 23/11	18 46 33.4	39.7000	19.1000	BAI	40.8770	17.2030	207.6	-	2.40688	2.38704	-	-	-
1974 335 01/12	12 09 28.8	39.5000	26.2000	BAI	40.8770	17.2030	780.9	-	2.54094	2.63278	-	-	-
1974 354 20/12	15 09 36.0	39.8000	20.5000	BAI	40.8770	17.2030	304.6	-	2.44344	2.45722	-	-	-
1975 016 16/01	00 09 47.1	38.2000	15.6000	BAI	40.8770	17.2030	327.6	-	2.44812	2.63815	-	-	-
1975 024 24/01	16 33 03.2	41.2000	19.7000	BAI	40.8770	17.2030	213.0	-	1.69000	2.03037	-	-	-
1975 025 25/01	14 14 09.3	38.0000	20.0000	BAI	40.8770	17.2030	400.0	-	2.14937	2.16333	-	-	-
1975 026 26/01	05 30 54.6	37.0000	24.5000	BAI	40.8770	17.2030	764.8	-	2.58344	2.65685	-	-	-
1975 066 07/03	04 13 05.1	45.9000	26.6000	BAI	40.8770	17.2030	943.0	-	2.37250	2.49926	-	-	-
1975 094 04/04	05 16 16.2	38.1000	22.0000	BAI	40.8770	17.2030	515.0	-	2.56562	2.64074	-	-	-
1975 174 23/06	13 17 38.4	50.6000	9.90000	BAI	40.8770	17.2030	1219.6	-	2.63281	2.74648	-	-	-
1975 259 16/09	18 45 47.4	41.5000	19.2000	BAI	40.8770	17.2030	181.3	-	1.50469	1.94019	-	-	-
1975 260 17/09	23 04 07.1	36.4000	23.1000	BAI	40.8770	17.2030	714.2	-	2.59344	2.61204	-	-	-
1975 265 22/09	00 44 57.7	35.3000	26.2000	BAI	40.8770	17.2030	1002.1	-	2.67219	2.69056	-	-	-
1975 294 21/10	23 01 22.8	43.1000	17.4000	BAI	40.8770	17.2030	247.4	-	2.37188	2.55556	-	-	-
1975 299 26/10	07 12 26.6	40.0000	35.0000	BAI	40.8770	17.2030	1510.6	-	2.69531	2.91685	-	-	-
1975 316 12/11	09 03 49.5	36.4000	28.2000	BAI	40.8770	17.2030	1077.6	-	2.97375	3.04370	-	-	-
1975 317 13/11	03 07 26.6	33.6000	22.9000	BAI(*)	40.8770	17.2030	952.2	2.21000	2.16597	2.20281	2.84226	3.09000	3.35000
1975 320 16/11	13 04 24.4	44.7000	9.60000	BAI	40.8770	17.2030	752.7	-	1.98719	2.23759	-	-	-
1978 143 23/05	23 34 11.4	40.7000	23.2000	MLT(*)	35.9000	14.4800	929.7	-	2.71804	2.73000	3.02032	3.26000	3.35144

1978 361 27/12	17 46 11.9	41.1000	13.6000	MLT	35.9000	14.4800	582.3	-	2.56875	2.75185	-	-	-
1979 020 20/01	13 50 01.9	38.7000	12.9000	MLT	35.9000	14.4800	340.8	-	2.13125	2.44815	-	-	-
1979 148 28/05	09 27 33.2	36.4000	31.9000	MLT(*)	35.9000	14.4800	1566.6	-	2.90460	2.85000	3.03885	3.19402	3.36691
1979 204 23/07	11 42 02.8	35.7000	26.4000	MLT(*)	35.9000	14.4800	1077.0	-	2.49755	2.80788	3.03712	3.34418	3.43000

Table A.3: List of events collected from Mantovani et al. (1985) and from Yanovskaya et al. (1990) (the events with the asterisk).

Date	O. Time	Event		Station			Km	Group Velocity (km/s) at different Periods (10s-35s)					
Y.-J.D.-G.D.	H-m-s	Lat.	Long.	Code	Lat.	Long.	Ev.-St.	10s	15s	20s	25s	30s	35s
1977 019 19/01	20 46 53.3	36.6000	08.5000	NPL	40.8460	14.2570	687.3	2.49000	3.00000	3.33000	3.54000	3.59000	3.62000
1973 329 25/11	04 20 22.5	36.2000	04.5000	NPL	40.8460	14.2570	994.1	2.52000	3.15000	3.42000	3.55000	3.61000	-
1973 328 24/11	14 05 46.4	36.1000	04.4000	NPL	40.8460	14.2570	1007.7	-	3.08000	3.42000	3.51000	3.64000	3.74000
1973 328 24/11	15 22 09.8	36.1000	04.4000	NPL	40.8460	14.2570	1007.7	2.46000	3.21000	3.43000	-	-	-
1974 171 20/06	17 08 27.3	46.0000	15.5000	NPL	40.8460	14.2570	581.4	2.12000	2.24000	2.36000	2.57000	2.79000	-
1976 128 07/05	00 23 50.4	46.2000	13.3000	NPL	40.8460	14.2570	599.8	2.30000	2.24000	2.57000	2.70000	2.95000	3.27000
1974 293 20/10	11 25 55.3	39.7000	18.9000	GSO	42.7520	11.1160	735.0	2.25000	2.45000	2.66000	3.00000	3.15000	3.43000
1976 362 27/12	07 54 13.3	39.1000	20.6000	NPL	40.8460	14.2570	575.3	2.38000	2.33000	2.47000	2.71000	3.01000	3.14000
1974 087 28/03	21 32 35.3	37.1000	15.0000	NPL	40.8460	14.2570	420.8	2.50000	2.50000	2.91000	3.30000	3.47000	-
1976 333 28/11	19 25 17.3	37.3000	20.3000	NPL	40.8460	14.2570	654.3	2.03000	2.08000	2.38000	2.78000	2.93000	3.05000
1974 293 20/10	11 25 55.3	39.7000	18.9000	NPL	40.8460	14.2570	414.8	2.38000	2.25000	2.38000	2.62000	3.00000	3.30000
1972 331 26/11	16 03 11.8	43.0000	13.4000	TNO	45.0580	07.6970	511.0	1.74000	1.98000	2.07000	2.15000	2.39000	2.65000
1972 035 04/02	02 42 18.9	43.8000	13.3000	TNO	45.0580	07.6970	467.4	1.68000	1.87000	-	-	-	-
1975 094 04/04	05 16 16.2	38.1000	22.0000	TNO	45.0580	07.6970	1418.1	1.98000	2.13000	2.40000	2.71000	2.97000	3.18000
1976 053 22/02	12 02 54.8	39.5000	22.2000	TNO	45.0580	07.6970	1343.5	2.06000	2.13000	2.38000	2.82000	3.03000	3.25000
1976 018 18/01	15 10 32.7	38.9000	20.6000	TNO	45.0580	07.6970	1267.1	1.95000	2.13000	2.37000	2.68000	3.12000	3.26000
1976 164 12/06	00 59 16.9	37.5000	20.6000	TNO	45.0580	07.6970	1365.8	2.05000	2.12000	2.41000	2.56000	3.02000	3.27000
1972 167 15/06	00 33 23.6	38.3000	22.2000	TNO	45.0580	07.6970	1418.7	1.99000	2.19000	2.38000	2.74000	3.11000	3.28000
1974 180 29/06	01 06 58.6	36.7000	05.2000	TNO	45.0580	07.6970	951.6	2.25000	3.13000	3.49000	3.72000	3.78000	-
1974 179 28/06	11 09 40.2	36.6000	05.3000	TNO	45.0580	07.6970	960.6	2.37000	3.15000	3.50000	3.70000	-	-
1973 328 24/11	14 05 46.4	36.1000	04.4000	TNO	45.0580	07.6970	1032.9	2.36000	3.17000	3.50000	3.62000	3.72000	3.87000
1973 328 24/11	15 22 09.8	36.1000	04.4000	TNO	45.0580	07.6970	1032.9	2.32000	3.10000	3.47000	3.63000	3.70000	3.86000
1973 329 25/11	04 20 22.5	36.2000	04.5000	TNO	45.0580	07.6970	1019.9	2.25000	3.04000	3.50000	3.65000	3.73000	-
1973 103 13/04	08 12 15.4	39.1000	17.0000	TNO	45.0580	07.6970	1014.0	-	2.09000	2.20000	2.38000	-	-
1976 128 07/05	00 23 50.4	46.2000	13.3000	TNO	45.0580	07.6970	454.9	2.00000	2.27000	-	-	-	-
1973 220 08/08	14 36 11.0	40.8000	15.4000	TNO	45.0580	07.6970	786.3	2.02000	2.09000	2.23000	2.40000	2.64000	2.72000
1976 362 27/12	07 54 13.3	39.1000	20.6000	BOL	44.4900	11.3290	974.7	2.30000	2.23000	2.47000	2.69000	2.97000	3.19000
1976 062 02/03	19 41 36.4	40.7000	19.7000	BOL	44.4900	11.3290	805.2	2.20000	2.35000	2.71000	3.00000	-	-
1975 094 04/04	05 16 16.2	38.1000	22.0000	BOL	44.4900	11.3290	1139.6	2.30000	2.20000	2.49000	2.72000	3.13000	3.25000
1973 328 24/11	14 05 46.4	36.1000	04.4000	BOL	44.4900	11.3290	1101.3	2.17000	2.77000	3.34000	3.49000	3.64000	3.69000
1973 328 24/11	15 22 09.8	36.1000	04.4000	BOL	44.4900	11.3290	1101.3	2.24000	2.77000	3.36000	3.49000	3.68000	3.74000
1973 329 25/11	04 20 22.5	36.2000	04.5000	BOL	44.4900	11.3290	1087.2	2.25000	2.80000	3.42000	3.49000	3.69000	3.72000
1972 140 19/05	01 13 43.5	35.2000	09.1000	BOL	44.4900	11.3290	1048.8	2.45000	2.73000	3.15000	3.35000	3.53000	3.67000
1972 331 26/11	16 03 11.8	43.0000	13.4000	BOL	44.4900	11.3290	235.0	1.76000	1.93000	2.15000	2.36000	2.48000	2.67000
1974 171 20/06	09 28 33.4	44.4000	17.7000	BOL	44.4900	11.3290	507.2	2.23000	2.14000	2.39000	2.65000	-	-
1974 171 20/06	17 08 27.3	46.0000	15.5000	BOL	44.4900	11.3290	367.9	2.02000	2.09000	2.28000	2.44000	2.62000	2.67000
1974 293 20/10	11 25 55.3	39.7000	18.9000	OLB	40.9260	09.4950	810.6	2.37000	2.84000	2.96000	3.18000	3.30000	3.58000
1976 053 22/02	12 02 54.8	39.5000	22.2000	OLB	40.9260	09.4950	1092.1	2.44000	2.77000	2.86000	3.10000	3.34000	3.55000
1976 062 02/03	19 41 36.4	40.7000	19.7000	OLB	40.9260	09.4950	860.9	2.47000	2.76000	2.94000	3.10000	3.33000	3.44000
1976 128 07/05	00 23 50.4	46.2000	13.3000	OLB	40.9260	09.4950	661.5	2.10000	2.57000	2.89000	3.08000	3.23000	3.43000
1976 132 11/05	22 44 00.2	46.3000	13.0000	OLB	40.9260	09.4950	660.5	2.16000	2.65000	2.95000	3.17000	3.22000	3.48000
1974 302 29/10	01 05 15.5	44.6000	18.4000	OLB	40.9260	09.4950	834.7	2.45000	2.60000	2.72000	2.97000	3.31000	-
1974 097 07/04	14 22 47.1	34.8000	24.7000	OLB	40.9260	09.4950	1497.9	2.37000	2.60000	2.76000	2.94000	3.10000	-

1975 094 04/04	05 16 16.2	38.1000	22.0000	OLB	40.9260	09.4950	1119.1	-	-	2.83000	3.00000	3.27000	3.45000
1976 122 01/05	05 10 25.1	37.8000	15.0000	OLB	40.9260	09.4950	587.6	2.40000	2.82000	3.03000	3.12000	3.20000	3.25000
1972 035 04/02	02 42 18.9	43.8000	13.3000	BLZ	46.5040	11.3460	337.5	1.93000	2.12000	2.40000	2.82000	3.25000	3.48000
1972 035 04/02	17 19 29.5	43.8000	13.3000	BLZ	46.5040	11.3460	337.5	1.92000	2.13000	2.37000	2.94000	-	-
1972 036 05/02	01 26 32.3	43.8000	13.3000	BLZ	46.5040	11.3460	337.5	1.90000	2.15000	2.33000	3.00000	3.26000	-
1973 328 24/11	14 05 46.4	36.1000	04.4000	BLZ	46.5040	11.3460	1292.4	2.15000	2.90000	3.27000	3.68000	-	-
1973 328 24/11	15 22 09.8	36.1000	04.4000	BLZ	46.5040	11.3460	1292.4	2.16000	2.87000	3.28000	3.52000	3.61000	3.67000
1976 164 12/06	00 59 16.9	37.5000	20.6000	BLZ	46.5040	11.3460	1258.3	2.32000	2.43000	2.65000	2.97000	3.35000	3.44000
1974 097 07/04	14 22 47.1	34.8000	24.7000	BLZ	46.5040	11.3460	1717.0	2.41000	2.49000	2.63000	2.89000	3.17000	3.27000
1974 302 29/10	01 05 15.5	44.6000	18.4000	GSO	42.7520	11.1160	622.0	2.40000	2.52000	2.61000	2.82000	3.10000	3.35000
1973 220 08/08	14 36 11.0	40.8000	15.4000	BLZ	46.5040	11.3460	712.9	1.91000	1.96000	2.46000	2.89000	3.18000	3.06000
1974 125 05/05	06 09 19.2	35.0000	04.6000	PAL	38.1430	13.3470	856.6	2.30000	2.54000	2.74000	3.08000	3.40000	3.60000
1974 124 04/05	15 14 11.9	34.8000	05.1000	PAL	38.1430	13.3470	826.6	2.25000	2.53000	2.69000	3.05000	3.43000	3.57000
1973 329 25/11	04 20 22.5	36.2000	04.5000	PAL	38.1430	13.3470	814.4	-	2.83000	3.00000	3.30000	3.45000	3.65000
1973 328 24/11	14 05 46.4	36.1000	04.4000	PAL	38.1430	13.3470	826.4	2.47000	2.84000	2.90000	3.15000	3.32000	3.62000
1973 328 24/11	15 22 09.8	36.1000	04.4000	PAL	38.1430	13.3470	826.4	2.47000	2.79000	2.94000	3.28000	3.37000	-
1974 097 07/04	14 22 47.1	34.8000	24.7000	PAL	38.1430	13.3470	1082.1	2.09000	2.21000	2.39000	2.74000	3.00000	3.25000
1974 293 20/10	11 25 55.3	39.7000	18.9000	PAL	38.1430	13.3470	511.6	2.18000	2.47000	-	-	-	-
1975 094 04/04	05 16 16.2	38.1000	22.0000	PAL	38.1430	13.3470	758.5	2.13000	2.30000	2.52000	2.90000	3.06000	3.30000
1976 128 07/05	00 23 50.4	46.2000	13.3000	GSO	42.7520	11.1160	420.7	2.06000	2.23000	2.47000	2.83000	3.01000	-
1976 132 11/05	22 44 00.2	46.3000	13.0000	GSO	42.7520	11.1160	421.7	2.08000	2.28000	2.56000	2.85000	3.03000	3.12000
1976 128 07/05	00 23 50.4	46.2000	13.3000	GSO	42.7520	11.1160	420.7	2.12000	2.17000	2.52000	2.75000	2.95000	-
1975 094 04/04	05 16 16.2	38.1000	22.0000	GSO	42.7520	11.1160	1057.1	2.27000	2.47000	2.58000	2.82000	3.12000	3.35000
		46.2200	13.3300	(*)	37.9700	23.7200	1254.2	2.44000	2.57000	2.72000	2.87000	3.01000	-
		46.2200	12.2000	(*)	37.9700	23.7200	1319.5	2.39000	2.48000	2.60000	2.83000	3.09000	-
		38.5500	27.6600	(*)	45.7090	13.7640	1394.1	3.02000	3.09000	2.98000	3.25000	3.42000	-

Appendix B. Phase Velocity Data.

In the following Table B.1 are listed the station-station paths and the values of the phase velocity, calculated through interpolation at different periods in the period range of 25s-100s. Data are collected from: Berry and Knopoff (1967), Calcagnile et al. (1979), Calcagnile and Panza (1979), Calcagnile and Panza (1980), Calcagnile et al. (1982), Calcagnile et al. (1984), Caputo et al. (1976), Knopoff et al. (1966), Knopoff et al. (1967), Panza (1976), Panza et al. (1978), Panza et al. (1982), Scalera et al. (1981), Yanovskaya et al.(1990).

Table B.1: List of station-station paths and associated Phase Velocity: code, latitude and longitude of the two stations of each station-station path, and the Phase Velocity values at different periods (25s-100s).

Station 1			Station 2			Phase Velocity (km/s) at different Periods (25s-100s)					
Code	Lat.	Long.	Code	Lat.	Long.	25s	30s	35s	50s	80s	100s
CHU	46.850	9.530	BES	47.250	5.980	3.600	3.680	3.760	3.860	3.895	-
AQU	42.354	13.405	TNO	45.060	7.697	3.547	3.577	3.651	3.804	3.992	4.012
ARK	54.680	13.435	MOX	50.646	11.616	3.809	3.840	3.892	4.030	-	-
OLB	40.927	9.495	TRI	45.709	13.764	3.470	3.682	3.760	3.820	3.944	4.020
TNO	45.060	7.697	BAI	40.877	17.203	3.510	3.622	3.697	3.910	4.030	-
TRI	45.709	13.764	AQU	42.354	13.405	3.750	3.868	3.900	3.930	3.983	4.072
BAI	40.877	17.203	TRI	45.709	13.764	3.740	3.848	3.885	3.950	3.990	4.068
CUG	40.190	8.570	ALG	36.770	3.060	-	3.800	3.804	3.850	-	-
CHU	46.850	9.530	BES	47.250	5.980	3.650	3.725	3.800	3.875	3.900	-
TOR	40.820	0.490	CUG	40.190	8.570	-	3.675	3.925	4.050	3.986	-
MON	43.730	7.430	TOR	40.820	0.490	-	3.675	3.795	4.000	-	-
MON	43.730	7.430	ALG	36.770	3.060	3.855	3.851	3.849	3.860	3.940	4.080
MON	43.730	7.430	BES	47.250	5.980	3.480	3.682	3.826	-	-	-
CUG	40.190	8.570	MON	43.730	7.430	-	-	-	3.970	4.010	-
BLZ	46.505	11.3468	TMO	45.060	7.697	-	3.650	3.765	3.962	4.050	4.087
ATU	37.972	23.717	AQU	42.354	13.405	-	-	3.745	3.880	3.971	4.040
IST	41.045	28.996	AQU	42.354	13.405	-	-	-	3.900	4.000	4.040
IST	41.045	28.996	ATU	37.972	23.717	-	-	3.860	3.960	4.050	4.100
PLR	38.144	13.3476	BAI	40.877	17.203	3.700	3.741	3.781	3.880	3.950	-
SBS	36.8666	10.350	NPL	40.8467	14.2578	3.650	3.693	3.735	3.850	4.000	-
NPL	40.8467	14.2578	TNO	45.060	7.697	3.500	3.574	3.646	3.830	4.000	-
PSZ	45.646	13.779	TTE	47.9184	19.8945	3.610	3.690	3.740	3.800	3.970	4.100

Appendix C. Non-linear Inversion Data.

In the following Tables (C.1, C.2, C.3), group and phase mean velocity data and their single point errors and R.M.S., parametrization and variability range of parameters are plotted for five out of the seven main regions, of our regionalization, studied by the non-linear inversion.

Table C.1: The phase mean velocity (from 30s to 100s) and group mean velocity (from 10s to 35s) values are plotted for some regions, five out of the seven main regions of our regionalization, studied by non-linear inversion. The measurement error is associated to each group velocity. The error associated to the phase velocity is equal at each period in the period range of 30-100s, and is been estimated considering Caputo et al. (1976). The R.M.S. values of group and phase velocity are plotted. In Region III the error and the R.M.S. values, associated to the phase velocity, is twice because there aren't any station-station paths crossing that region.

	REGION I				REGION III				REGION IV			
Period (s)	Vph (km/s)	Error (km/s)	Vg (km/s)	Error (km/s)	Vph (km/s)	Error (km/s)	Vg (km/s)	Error (km/s)	Vph (km/s)	Error (km/s)	Vg (km/s)	Error (km/s)
100	3.983	0.060			3.998	0.120			3.982	0.060		
80	3.940	0.060			3.941	0.120			3.935	0.060		
50	3.837	0.060			3.868	0.120			3.867	0.060		
35	3.714	0.060	3.391	0.140	3.789	0.120	3.110	0.140	3.759	0.060	3.261	0.140
30	3.665	0.060	3.244	0.080	3.738	0.120	3.002	0.080	3.718	0.060	3.079	0.080
25			3.045	0.070			2.856	0.070			2.833	0.070
20			2.914	0.070			2.706	0.070			2.579	0.070
15			2.758	0.080			2.646	0.080			2.385	0.080
10			2.515	0.100			2.570	0.100			2.337	0.100
R.M.S.	0.035		0.060		0.070		0.060		0.035		0.060	

	REGION V				REGION VII			
Period (s)	Vph (km/s)	Error (km/s)	Vg (km/s)	Error (km/s)	Vph (km/s)	Error (km/s)	Vg (km/s)	Error (km/s)
100	3.979	0.060			3.979	0.060		
80	3.944	0.060			3.922	0.060		
50	3.845	0.060			3.851	0.060		
35	3.719	0.060	3.056	0.140	3.750	0.060	3.468	0.140
30	3.660	0.060	2.888	0.080	3.681	0.060	3.294	0.080
25			2.638	0.070			3.024	0.070
20			2.430	0.070			2.809	0.070
15			2.207	0.080			2.689	0.080
10			2.113	0.100			2.460	0.100
R.M.S.	0.035		0.060		0.035		0.060	

Table C.2: The structural model (thickness, S-wave and P-wave velocity) considered fixed for the upper crust and the parametrization used in the lower crust and in the mantle are plotted for five out of the seven main regions of our regionalization. The structure below the last indicated layer is fixed and equal for all the five regions. The parameters P_i, with i = 1, 2, 3, 4, 5, represent thickness-parameters (in km) of the layers; the parameters P_i, with i = 6, 7, 8, 9, 10, represent S-wave velocity-parameters (in km/s) of the layers.

REGION I		
Thickness (km)	Vs (km/s)	Vp (km/s)
3.0	0.00	1.52
0.7	1.20	2.00
1.0	3.40	5.90
2.0	4.00	6.90
P01	P06	1.73xP06
P02	P07	1.73xP07
P03	P08	1.73xP08
P04	P09	1.73xP09
P05	P10	1.73xP10
342.3-ΣP_i	4.60	7.95

REGION III		
Thickness (km)	Vs (km/s)	Vp (km/s)
6.0	2.95	5.10
4.0	3.00	5.20
P01	P06	1.73xP06
P02	P07	1.73xP07
P03	P08	1.73xP08
P04	P09	1.73xP09
P05	P10	1.73xP10
339-ΣP_i	4.60	7.95

REGION IV		
Thickness (km)	Vs (km/s)	Vp (km/s)
1.0	0.00	1.52
1.0	1.70	2.94
4.0	2.40	4.15
5.0	3.30	5.70
P01	P06	1.73xP06
P02	P07	1.73xP07
P03	P08	1.73xP08
P04	P09	1.73xP09
P05	P10	1.73xP10
338-ΣP_i	4.60	7.95

REGION V		
Thickness (km)	Vs (km/s)	Vp (km/s)
1.1	1.50	2.65
2.4	2.10	3.60
4.0	2.90	5.00
2.0	3.25	6.05
P01	P06	1.73xP06
P02	P07	1.73xP07
P03	P08	1.73xP08
P04	P09	1.73xP09
P05	P10	1.73xP10
339.5-ΣP_i	4.60	7.95

REGION VII		
Thickness (km)	Vs (km/s)	Vp (km/s)
6.0	2.70	4.67
6.0	3.00	5.20
P01	P06	1.73xP06
P02	P07	1.73xP07
P03	P08	1.73xP08
P04	P09	1.73xP09
P05	P10	1.73xP10
337-ΣP_i	4.60	7.95

Table C.3: The variability range and step for each parameter P_i (with i = 1, ..., 10) are plotted for some regions, five out of the seven main regions of our regionalization, studied by non-linear inversion.

	REGION I		REGION III		REGION IV		REGION V		REGION VII	
Parameter	Range	Step	Range	Step	Range	Step	Range	Step	Range	Step
Thickness	(km)	(km)	(km)	(km)	(km)	(km)	(km)	(km)	(km)	(km)
P01	5-25	5	5-25	10	8-20	6	5-11	3	13-23	10
P02	4-28	8	10-40	30	10-50	20	5-25	10	15-65	25
P03	15-65	25	5-45	20	20-70	50	15-40	25	20-70	50
P04	25-75	50	35-85	25	15-65	25	60-130	70	30-70	40
P05	45-145	100	30-140	55	25-125	50	60-130	70	40-100	60
Velocity	(km/s)	(km/s)	(km/s)	(km/s)	(km/s)	(km/s)	(km/s)	(km/s)	(km/s)	(km/s)
P06	3.00-4.75	0.25	2.60-4.40	0.15	2.75-4.25	0.10	2.00-4.40	0.15	3.05-4.45	0.20
P07	2.80-4.80	0.20	2.80-4.90	0.30	3.70-4.75	0.15	3.15-4.50	0.15	3.50-4.70	0.40
P08	3.10-5.10	0.50	4.00-5.10	0.25	4.00-5.05	0.30	3.40-4.80	0.20	4.05-4.85	0.20
P09	3.90-4.80	0.30	4.05-4.85	0.20	4.00-4.70	0.40	4.00-4.80	0.20	4.00-4.80	0.40
P10	4.00-4.75	0.25	4.00-4.90	0.30	4.00-4.90	0.30	4.00-4.90	0.30	4.00-4.80	0.40

References.

Ahrens, T.J., 1973. Petrologic properties of the upper 670 km of the Earth's mantle; geophysical implications. Phys. Earth Planet. Inter., 7: 167-186.

Amato, A., Chiarabba, C., and Selvaggi, G., 1997. Crustal and deep seismicity in Italy (30 years after). Ann. Geophys., 40: 981-994.

Anderson, H., and Jackson, J., 1987. Active tectonics of the Adriatic Region. Geophys. J. R. Astr. Soc., 91: 937-983.

Backus, G., and Gilbert, J.F., 1968. Resolving power of gross earth data. Geophys. J. R. Astr. Soc., 16: 168-205.

Backus, G., and Gilbert, J.F., 1970. Uniqueness in the inversion of inaccurate gross earth data. Phil. Trans. R. Soc. A., 266: 123-192.

Bally, A.W., Burbi, L., Cooper, C., and Ghelardoni, R., 1986. Balanced sections and seismic reflection profiles across the Central Apennines. Mem. Soc. Geol. It., 35: 257-310.

Barchi, M.R., De Feyter, A., Magnani, M.B., Minelli, G., Pialli, G., and Sotera, B.M., 1998. The structural style of the Umbria-Marche fold and thrust belt. Mem. Soc. Geol. It., 52: 557-578.

Berry, M.J., and Knopoff, L., 1967. Structure of the Upper Mantle under the Western Mediterranean Basin. Journal of Geophysical Research, 72, pp. 3613-3626.

Bondar, I., Bus, Z., Zivcic, M., Costa, G., and Levshin, A., 1995. Rayleigh wave group and phase velocity measurements in the Pannonian Basin. XV Congress of the Carpatho-Balcan Geologica Association.

Bottinga, Y., and Steinmetz, L., 1979. A geophysical, geochemical, petrological model of the sub-marine lithosphere. Tectonophysics, 55: 311-347.

Calcagnile, G., Panza, G.F., and Knopoff, L., 1979. Upper mantle structure of North-Central Italy from Rayleigh waves phase velocities. Tectonophysics, 56, pp. 51-63.

Calcagnile, G., and Panza, G.F., 1979. Crustal and upper mantel structure beneath the Apennines region as inferred from the study of Rayleigh waves. J. Geophys., 45, pp. 319-327.

Calcagnile, G., and Panza, G.F., 1980. Upper mantle structure of the Apulian plate from Rayleigh waves. Pageoph, 118, pp. 823-830.

Calcagnile, G., and Panza, G.F., 1981. The main characteristics of the lithosphere-astenosphere system in Italy and surronding regions. Pure Appl. Geophys., 119: 865-879.

Calcagnile, G., D'Ingeo, F., Farrugia, P., and Panza, G.F., 1982. The lithosphere in the central-eastern Mediterranea area. Pure Appl. Geophys., 120: 389-406.

Calcagnile, G., Mascia, U., Del Gaudio, V., and Panza, G.F., 1984. Deep structure of southeastern Europe from Rayleigh waves.}} Tectonophysics, 110, pp. 189-200.

Caputo, M., Knopoff, L., Mantovani, E., Mueller, S., and Panza, G.F., 1976. Rayleigh waves phase velocities and upper mantle structure in the Apennines. Ann. Geof., 29, pp. 199-214.

Catalano, R., Doglioni, C., and Merlini, S., 2001. On the Mesozoic Ionian Basin. Geophys. J. Int., 144: 49-64.

Cattaneo, M., Augliera, P., Parolai, S., and Spallarossa, D., 1999. Anomalously deep earthquakes in northwestern Italy. J. Seismol., 3: 421-435.

Della Vedova, B., Marson, I., Panza, G.F., and Suhadolc, P., 1991. Upper mantle properties of the Tuscan-Tyrrhenian area: a framework for its recent tectonic evolution. Tectonophysics, 195: 311-318.

Ditmar, P.G., and Yanovskaya, T.B., 1987. A generalization of the Backus-Gilbert method for estimation of lateral variations of surface wave velocity. Izv. AN SSSR, Fiz. Zemli (Physics of the Solid Earth), 23 (6): 470-477.

Du, Z.J., Michelini, A., and Panza, G.F., 1998. EurID: a regionalised 3-D seismological model of Europe. Phys. Earth Planet. Inter., 105: 31-62.

Farrugia, P., and Panza, G.F., 1981. Continental character of the lithosphere beneathh the Ionian Sea. In: The solution of the Inverse Problem in Geophysical interpretation. Cassinis R. ed., Plenum Pub. Corp., 327-334.

Finetti, I., and Del Ben, A., 1986. Geophysical study of the Tyrrhenian opening. Boll. Geofis. Teor. Appl., 28, 110: 75-156.

Fowler, C.M.R., 1995. The Solid Earth. An introduction to Global Geophysics. Cambridge Univ. Press.

Graham, E.K., 1970. Elasticity and composition of the upper mantle. Geophys. J. R. Astr. Soc., 20: 285-302.

Karagianni, E.E., Panagiotopoulos, D.G., Panza, G.F., Suhadolc, P., Papazachos, C.B., Papazachos, B.C., Kiratzi, A., Hatzfeld, D., Makropoulos, K., Priestley, K., and Vuan, A., 2001. Rayleigh Wave Group Velocity Tomography in the Aegean area. Submitted to Tectonophysics.

Knopoff, L., Mueller, S., and Pilant, W.L., 1966. Structure of the crust and upper mantle in the Alps from the phase velocity of Rayleigh waves. Bulletin of the Seismological Society of America, 56, pp. 1009-1044.

Knopoff, L., Berry, M.J., and Schwab, F.A., 1967. Tripartite phase velocity observations in laterally heterogeneous regions. Journal of Geophysical Research, 72, pp. 2595-2601.

Knopoff, L., 1972. Observations and inversion of surface-wave dispersion. In: The Upper Mantle. Tectonophysics, Ritsema A.R. ed., 13 (1-4): 497-519.

Knopoff, L., and Panza, G.F., 1977. Resolution of Upper Mantle Structure using higher modes of Rayleigh waves. Annales Geophysicae , 30.

Laske, G., and Masters, G., 1997. A global digital map of sediment thickness. EOS Trans. AGU, 78, F483 (http://mahi.ucsd.edu/Gabi/sediment.html).

Lay, T., and Wallace, T.C., 1995. Modern Global Seismology. Dmowska R. and Holton J.R. eds., Academic Press, pp. 230.

Levshin, A.L., Pisarenko, V.F., and Pogrebinsky, G.A., 1972. On a frequency time analysis of oscillations. Annales Geophysicae, 28: 211-218.

Levshin, A.L., Ratnikova, L., and Berger, J., 1992. Peculiarities of surface wave propagation across Central Eurasia. Bull. Seismol. Soc. Am., 82: 2464-2493.

Mantovani, E., Nolet, G., and Panza, G.F., 1985. Lateral heterogeneity in the crust of the Italian region from regionalized Rayleigh-wave group velocities. Annales Geophysicae, 3: 519-530.

Meletti, C., Patacca, E., and Scandone, P., 2000. Construction of a Seismotectonic Model: The Case of Italy. Pure Appl. Geophys., 157: 11-35.

Panza, G.F., 1976. Phase velocity determination of fundamental Love and Rayleigh waves. Pageoph, 114, pp. 753-764.

Panza, G.F., Neunhofer, H., and Calcagnile, G., 1978. Contribution to phase velocity investigation of Rayleigh waves in Middle Europe. Pageoph, 116, pp. 1299-1306.

Panza, G.F., 1981. The resolving power of seismic surface waves with respect to crust and upper mantle structural models. In: The solution of the inverse problem in geophysical interpretation. Cassinis R. ed., Plenum Publ. Corp., 39-77.

Panza, G.F., Mueller, S., Calcagnile, G., and Knopoff, L., 1982. Delineation of the north central Italian upper mantle anomaly. Nature, 296, pp. 238-239.

Pasyanos, M.E., Walter, W.R., and Hazler, S.E., 2001. A surface wave dispersion study of the Middle East and North Africa for Monitoring the Compressive Nuclear-Test-Ban Treaty. Pure Appl. Geophys., 158: 1445-1474.

Pepe, F., Bertotti, G., Cella, F., and Marsella, E., 2000. Rifted margin formation in the south Tyrrhenian Sea: a high-resolution seismic profile across the north Sicily passive continental margin. Tectonics, 19, 2: 241-257.

Ringwood, A.E., 1966. Mineralogy of the mantle. In: Advances in Earth Science. P.M. Hurley ed., MIT Press, 357-399.

Ritzwoller, M.H., and Levshin, A.L., 1998. Eurasian surface wave tomography: Group velocities. J. Geophys. Res., 103, B3: 4839-4878.

Scalera, G., Calcagnile, G., and Panza, G.F., 1981. Lateral variations of the "400-kilometers" discontinuity in the Mediterranean area. Boll. Geof. Teor. Appl., 23, pp. 11-16.

Trua, T., Serri, G., Marani, M.P., Renzulli, A., and Gamberi, F., 2001. Volcanological and petrological evolution of Marsili Seamount (Southern Tyrrhenian Sea). Eug XI, Strasbourg (France), April 2001.

Urban, L., Cichowicz, A., and Vaccari, F., 1993. Computation of analytical partial derivatives of phase and group velocities for Rayleigh waves with respect to structural parameters. Studia geoph. et geod., 37: 14-36.

Valyus, V.P., Keilis-Borok, V.I., and Levshin, A., 1969. Determination of the upper-mantle velocity cross-section for Europe. Proc. Acad. Sci. USSR, 185, 3.

Valyus, V.P., 1972. Determining seismic profiles from a set of observations. In: Computational Seismology. Keilis-Borok ed., Consult. Bureau, New-York, 114-118.

Vuan, A., Russi, M., and Panza, G.F., 2000. Group velocity tomography in the Subantartic Scotia Sea region. Pure Appl. Geophys., 157: 1337-1357.

Yanovskaya, T.B., 1982. Distribution of surface wave group velocities in the North Atlantic. Izv. AN SSSR, Fiz. Zemli, 2: 3-11.

Yanovskaya, T.B., Maaz, R., Ditmar, P.G., and Neunhofer, H., 1988. A method for joint interpretation of the phase and group surface-wave velocities to estimate lateral variations of the Earth's structure. Phys. Earth Planet. Inter., 51: 59-67.

Yanovskaya, T.B., and Ditmar, P.G., 1990. Smoothness criteria in surface-wave tomography. Geophys. J. Int., 102: 63-72.

Yanovskaya, T.B., Panza, G.F., Ditmar, P.D., Suhadolc, P., and Mueller, S., 1990. Structural heterogeneity and anisotropy based on 2-D phase velocity pattern of Rayleigh waves in Western Europe. Rend. Fis. Acc. Lincei, 9, 1: 127-135.

Yanovskaya, T.B., 1997. Resolution estimation in the problems of seismic ray tomography. Izv., Physics of the Solid Earth, 33, 9: 762-765.

Yanovskaya, T.B., Kizima, E.S., and Antonova, L.M., 1998. Structure of the crust in the Black Sea and adjoining regions from surface wave data. Journal of Seism., 2: 303-316.

Yanovskaya, T.B., and Antonova, L.M., 2000. Lateral variations in the structure of the crust and upper mantle in the Asian region from data on the group velocities of Rayleigh waves. Izv., Physics of the Solid Earth, 36, 2: 121-128.

Yanovskaya, T.B., Antonova, L.M., and Kozhevnikov, V.M., 2000. Lateral variations of the upper mantle structure in Eurasia from group velocities of surface waves. Phys. Earth Planet. Inter., 122: 19-32.

Zivcic, M., Bondar, I., and Panza, G.F., 2000. Upper crustal velocity structure in Slovenia from Rayleigh wave dispersion. Pure Appl. Geophys., 157: 131-146.